EVALUATION OF THE PROCEDURE USED TO DETERMINE NONLINEAR SOIL PROPERTIES IN SITU

A Thesis

by

DANIEL E. TORRES

Submitted to the Office of Graduate Studies of
Texas A&M University
in partial fulfillment of the requirements for the degree of

MASTER OF SCIENCE

December 2010

Major Subject: Civil Engineering

Evaluation of the Procedure Used to Determine Nonlinear Soil Properties In Situ

EVALUATION OF THE PROCEDURE USED TO DETERMINE NONLINEAR SOIL PROPERTIES IN SITU

A Thesis

by

DANIEL E. TORRES

Submitted to the Office of Graduate Studies of
Texas A&M University
in partial fulfillment of the requirements for the degree of

MASTER OF SCIENCE

Approved by:

Co-Chairs of Committee,	Giovanna Biscontin
	Jose M. Roesset
Committee Member,	J.N. Reddy
Head of Department,	John Niedzwecki

December 2010

Major Subject: Civil Engineering

ABSTRACT

Evaluation of the Procedure Used to Determine Nonlinear Soil Properties In Situ.

(December 2010)

Daniel E. Torres, B.S., Texas A&M University

Co-Chairs of Advisory Committee: Dr. Giovanna Biscontin
Dr. Jose M. Roesset

Soil properties (shear modulus and damping) are normally determined from laboratory tests. These tests provide both values of the shear modulus in the linear elastic range for very small levels of strain, and its variation with the level of strain. It has become more common to measure the maximum shear modulus at low levels of strain directly in the field, using geophysical techniques. The values obtained in situ can differ significantly in some cases from those determined in the laboratory, and a number of reasons and correction factors have been proposed in the literature to account for this variation. As a result, when in situ properties are available, it is normal to use these values for very low levels of strain, but still assume that the variation of the ratio G/G_{max} (normalized shear modulus) with shear strain is the same as determined in the laboratory.

Recently, tests have been performed using large vibrators (the Thumper and Tyrannosaurus Rex of the University of Texas at Austin) to determine soil properties in situ for larger strains, and the variation of G/G_{max} obtained from these tests has been

compared to that reported in the literature from lab tests. Observation indicates some generally good agreement, but also some minor variations. One must take into account, however, that in the determination of the shear modulus versus strain in the field from vibration records, a number of approximations are introduced. The objective of this work is to evaluate the accuracy of some the procedures used and to assess the validity of the simplifying assumptions which are made.

For this purpose, a shear cone that would reproduce correctly the horizontal stiffness of a circular mat foundation on the surface of an elastic, homogeneous half space, was considered. The cone was discretized using both a system of lumped masses and springs and a finite difference, using second-order central difference formulation, verifying that in the linear elastic range the results were accurate. A number of studies were conducted next, increasing the level of the applied force and using nonlinear springs that would reproduce a specified G/G_{max} vs. γ curve. Using a similar procedure to that used in the field tests, the shear wave velocity between hypothetical receivers and the levels of strain were determined. The resulting values of G/G_{max} vs. γ were then compared with the assumed curve to assess the accuracy of the estimated values.

ACKNOWLEDGEMENTS

I would like to thank my committee chair and co-chair, Dr. Jose Roesset and Dr. Giovanna Biscontin, and my committee member, Dr. J. N. Reddy, for their guidance and support throughout the course of this research.

Thanks also go to my friends and colleagues and the department faculty and staff, in particular to Dr. Luciana Barroso, Dr. Mark Burris and Dr. Terry Kohutek, for making my time at Texas A&M University a great experience.

Finally, thanks to my mother and father for their encouragement and to my sister for her support.

NOMENCLATURE

G	Shear Modulus
G_{MAX}	Maximum Shear Modulus
$\gamma = -\frac{du}{dz}$	Shear Strain
γ_{rz}	Shear Strain
γ_{xz}	Shear Strain
ρ	Mass Density
v	Poisson's Ratio
r_o	Circular Foundation Radius
c	Shear Wave Velocity
c_{MAX}	Maximum Shear Wave Velocity
Ω	Frequency
k	Horizontal Stiffness
u	Horizontal Displacement
$\lvert u \rvert$	Amplitude of Horizontal Displacement
z_o	Elevation of the Shear Cone Vertex above the Free Surface
z	Depth or Distance
r	Shear Cone Radius
A	Shear Cone Area

A_o	Initial Area
k_i	Spring Stiffness
V	Volume of Truncated Cone
P	Applied Force
A_{eq}	Equivalent Area
M	Total Mass
Δz	Mesh Size
f	Frequency
t	Time
τ	Stress Shear
$\tilde{\gamma}$	Average Shear Strain

TABLE OF CONTENTS

Page

ABSTRACT iii

ACKNOWLEDGEMENTS v

NOMENCLATURE vi

TABLE OF CONTENTS viii

LIST OF FIGURES x

LIST OF TABLES xii

1. INTRODUCTION 1

    1.1 Background 1
    1.2 Objectives and Organization 3

2. FORMULATION 9

    2.1 Introduction 9
    2.2 Analytical Formulation 10
    2.3 Spring and Mass Model 14
    2.4 Finite Difference Using Second-Order Central Difference Model 15
    2.5 Validation of the Discrete Models 17
        2.5.1 Displacements 17
        2.5.2 Strains 26

3. NONLINEAR ANALYSIS 29

    3.1 Soil Model 29
    3.2 Procedure 34
    3.3 Results 35

4. CONCLUSIONS 48

    4.1 Summary and Conclusions 48
    4.2 Further Studies 50

Page

REFERENCES 51

APPENDIX 54

VITA 67

LIST OF FIGURES

Page

Figure 1.1 G/Gmax vs. γ 2

Figure 1.2 Tests instrumentation (n.t.s.)..... 4

Figure 1.3 NEES equipment of University of Texas at the National Geotechnical Experimentation Site (NGES) located on the Texas A&M Riverside Campus 5

Figure 2.1 Cone Model..... 16

Figure 2.2 Displacement History--TOR 1 with Δz= 0.05 m f=50 Hz..... 17

Figure 2.3 Displacement History--TOR 1 with Δz= 0.10 m f=10 Hz..... 19

Figure 2.4 Displacement History--TOR 1 with Δz= 0.10 m f= 50 Hz..... 19

Figure 2.5 Displacement History--TOR 1 with Δz= 0.10 m f= 100 Hz..... 20

Figure 2.6 Displacement History--TOR 2 with Δz= 0.01 m f= 50 Hz..... 21

Figure 2.7 Displacement History--TOR 2 with Δz= 0.01 m f=10 Hz..... 23

Figure 2.8 Displacement History--TOR 2 with Δz= 0.01 m f=50 Hz..... 23

Figure 2.9 Displacement History--TOR 2 with Δz= 0.01 m f= 100 Hz..... 24

Figure 2.10 Comparison TOR 1 and TOR 2 with analytical solution as a function of Δz 25

Figure 2.11 Comparison of Strains for TOR 1 with Δz=0.10 m and 0.05 m, TOR2 with Δz=0.01 m and ANALY 28

Figure 3.1 $\frac{G}{G_{MAX}}$ vs. γ for springs selected 29

Page

Figure 3.2 $\frac{\tau}{G_{\max}}$ *vs.* γ for springs selected 32

Figure 3.3 $\frac{G}{G_{MAX}}$ vs. γ for springs selected 33

Figure 3.4 Shear Modulus Curve with Δz= 0.05 m and Δz= 0.10 m. 36

Figure 3.5 Shear Modulus Curve with $\frac{c^2}{c^2_{MAX}}$ for Δz= 0.10 m and Δz= 0.05 m 40

Figure 3.6 Shear Modulus Curve for $\frac{G}{G_{MAX}}$ vs. $\tilde{\gamma}$ with Δz= 0.10 m and Δz= 0.05 m 41

Figure 3.7 Shear Modulus Curve for $\frac{c^2}{c^2_{MAX}}$ vs. $\tilde{\gamma}$ 42

Figure 3.8 Displacement History--P=100 N with Δz= 0.10 m f= 50 Hz 43

Figure 3.9 Displacement History--P=500 N with Δz= 0.10 m f= 50 Hz 43

Figure 3.10 Displacement History--P=1,000 N with Δz= 0.10 m f= 50 Hz..... 44

Figure 3.11 Displacement History--P=5,000 N with Δz= 0.10 m f= 50 Hz..... 44

Figure 3.12 Displacement History--P=10,000 N with Δz= 0.10 m f= 50 Hz 45

Figure 3.13 Displacement History--P=100 N with Δz= 0.05 m f= 50 Hz..... 45

Figure 3.14 Displacement History--P=500 N with Δz= 0.05 m f= 50 Hz..... 46

Figure 3.15 Displacement History--P=1,000 N with Δz= 0.05 m f= 50 Hz..... 46

Figure 3.16 Displacement History--P=5,000 N with Δz= 0.05 m f= 50 Hz..... 47

LIST OF TABLES

Page

Table 2.1 Maximum Values for TOR 1 at different depths 18

Table 2.2 Maximum Values for TOR2 at different depths 22

Table 2.3 Results for TOR1, TOR2 and Analytical Solution 26

Table 2.4 Strains Values for TOR1, TOR2 and ANALY 27

Table 3.1 $\frac{\tau}{G_{\max}} vs. \gamma$ for springs selected 30

Table 3.2 Values for TOR1 Δz=0.1 m 38

Table 3.3 Values for TOR1A Δz=0.05 m 39

1. INTRODUCTION

1.1 Background

Soil properties measured in situ for very low levels of strain can differ significantly from those determined in the laboratory for two reasons: sample disturbance and time effects. Numerous studies have attempted to explain these differences and to provide correction factors that could be applied to the experimental data (Anderson and Woods, 1975). As a result it is common today, particularly in geotechnical earthquake engineering, to use when possible values of the shear modulus at low levels of strain determined in the field through geophysical methods, and to use on the other hand the variation of the modulus with level of strain from laboratory tests (cyclic tests). Figure 1.1 shows a typical variation of the shear modulus, divided by its maximum value, as a function of shear strain in log scale. The actual shape of this curve depends on the type of soil (sand, clays, very plastic clays) and is affected also by the state of stress (confining stress). Such curves have been proposed by Seed and Idriss (1970), Kim (1991), and Darendeli (2001) among many others. The basic assumption made for nonlinear seismic analyses is thus that both the relative variation of the shear modulus with strain level (dividing the modulus by its maximum value corresponding to very low levels of strain) and the variation of the damping would be the same for in situ and laboratory tests.

This thesis follows the style of *ASCE Geotechnical and Geoenvironmental Engineering*.

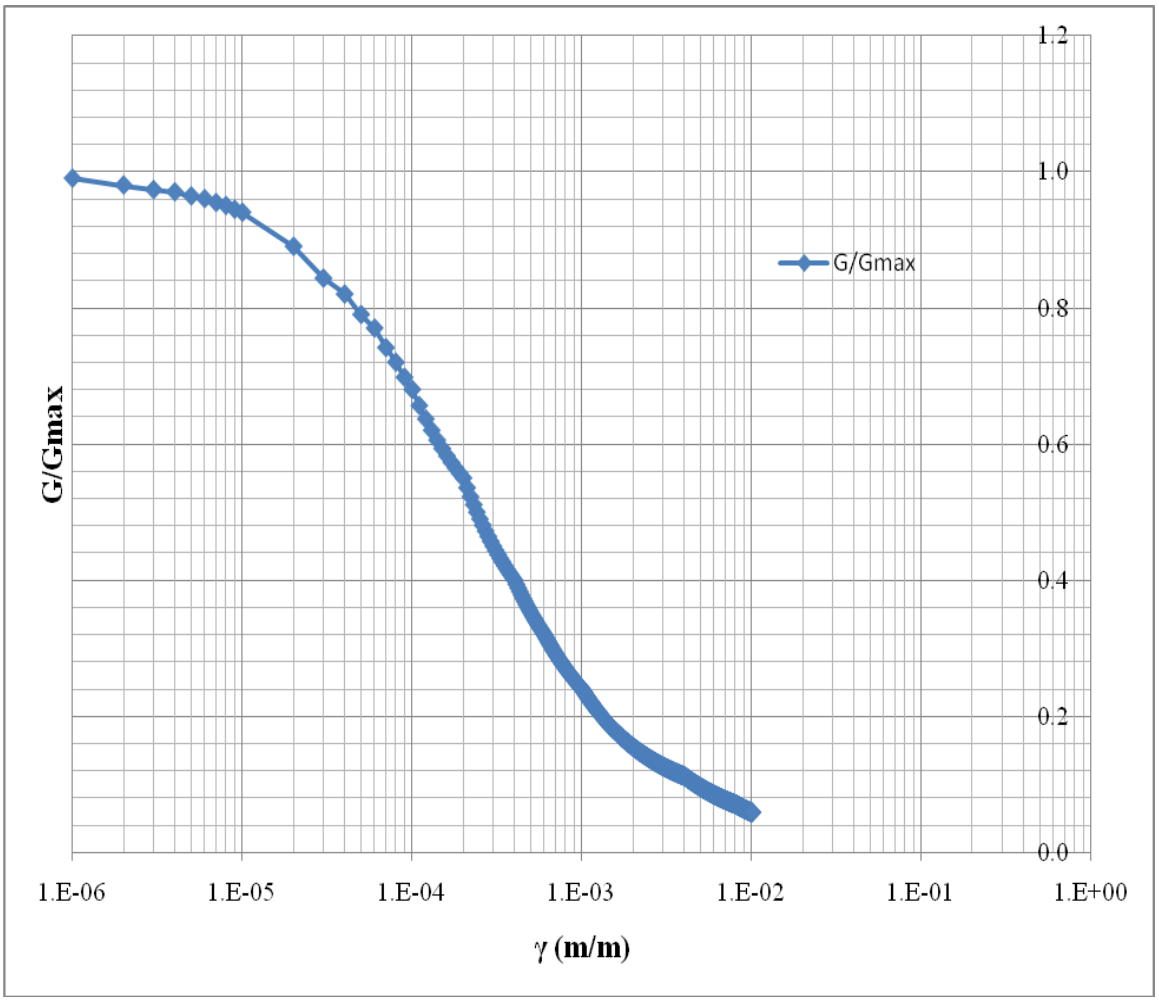

Figure. 1.1 $\frac{G}{G_{MAX}}$ vs. γ

More recent studies have raised some questions as to the accuracy of this approach. Until recently, it had been impossible to measure in situ shear modulus and damping for different levels of excitation. The recent development of special equipment at the University of Texas at Austin, under the NEES program, (Stokoe, Kurtulus and Park 2006, Park 2007) offers the opportunity to do so in a realistic manner but work is

needed on the interpretation of the data to obtain the desired properties. There is a scarcity of experimental data to help validate different approaches, formulations and models, and one must guarantee that when experimental studies are conducted in the field pertinent data are properly measured and interpreted. Laboratory tests have the advantage that the excitation and the system parameters can be controlled and measured accurately. They have the disadvantage by the same token that the controls can prevent the occurrence of an unexpected phenomenon that would, or could, in fact occur in the field.

Field tests are much more important from this point of view, particularly for geotechnical studies, because of the importance of the radiation of waves into the far field. One must be careful, however, to ensure that the instrumentation is as complete as possible and that the interpretation of the measured data does not introduce a bias to avoid reaching the wrong conclusions.

1.2 Objectives and Organization

The main objective of this study is to evaluate the accuracy of the procedure used in practice to determine nonlinear soil properties in situ in order to compare them to those reported in the literature from lab tests.

In tests performed at the University of Texas at Austin and at the Riverside campus of Texas A & M University using the dynamic testing equipment developed at the former under the auspices of the NEES program of the National Science Foundation,

a circular slab was placed on the ground and subjected to harmonic loads of different amplitudes (Figure 1.2 and 1.3). The resulting particle velocities at various depths under the slab were determined from an array of geophones and the corresponding displacements and strains computed. The corresponding value of the shear modulus was then determined from the time lag between the maximum values recorded at the different depths, computing first the shear wave velocity and then the modulus. Details of the experimental set up and of the measurements are provided in Ahn (2007). Ahn used then a numerical simulation with a 3D finite element discretization of the soil in cylindrical coordinates to reproduce theoretically the tests and to investigate the resulting variation of the modulus with level of strain.

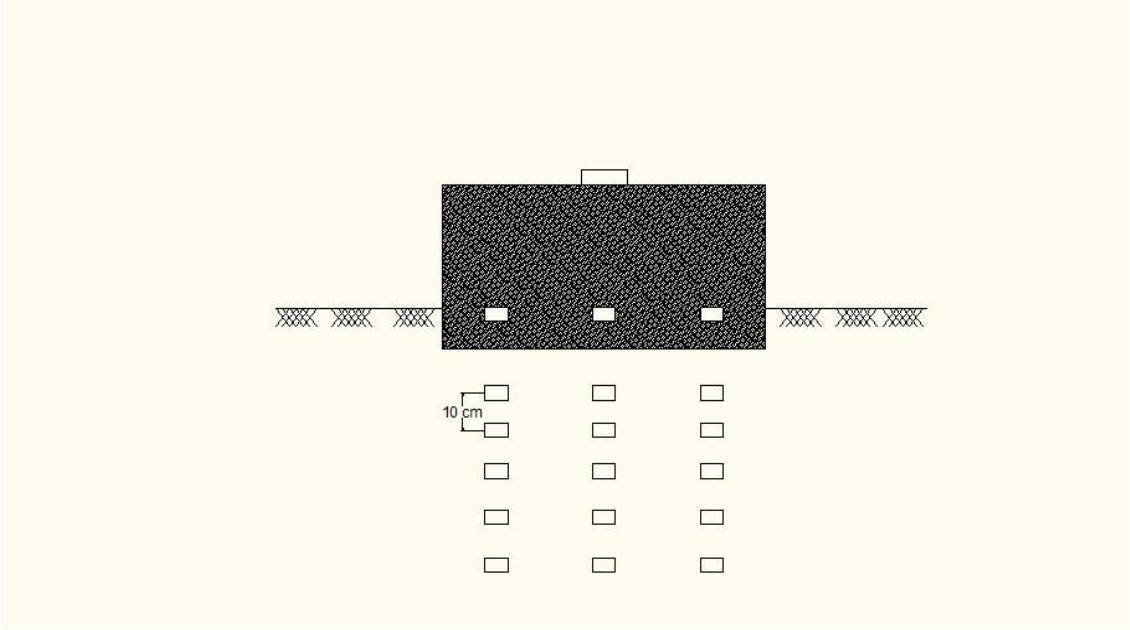

Figure 1.2 Tests instrumentation (n.t.s.)

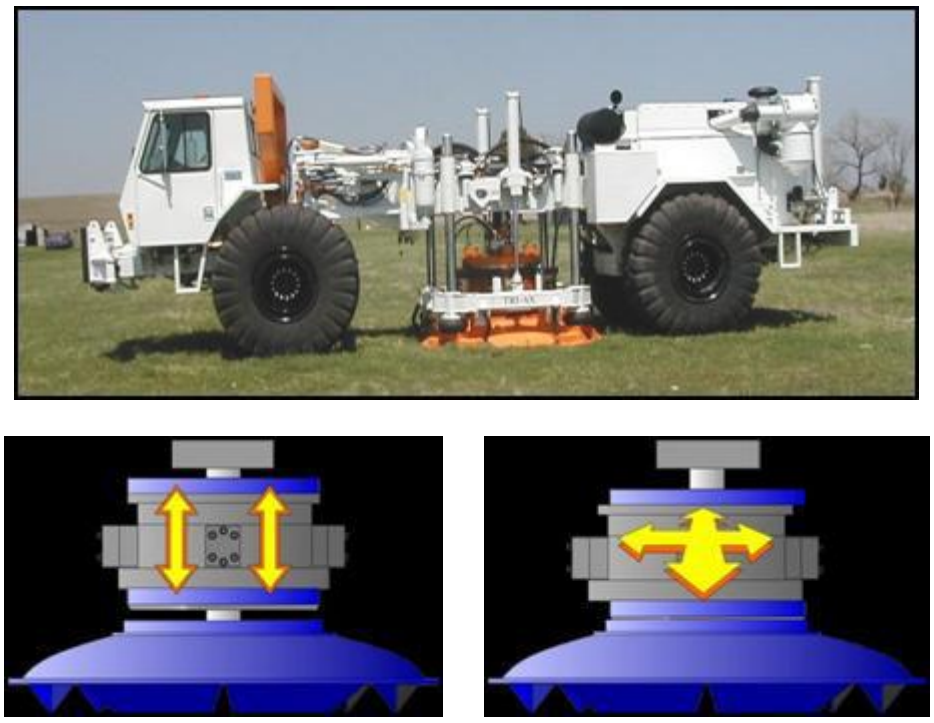

Figure 1.3 NEES equipment of University of Texas at the National Geotechnical Experimentation Site (NGES) located on the Texas A&M Riverside Campus

The procedure used to determine the variation of the modulus with the level of strain involves a number of approximations. It should be noticed first that while the traditional curves of G/Gmax versus γ assume a one dimensional pure shear condition this is not the case in the tests where there will be a more complex 3D state of strains. A question that could be raised then is what is the most appropriate value of shear strain to consider: the octahedral shear strain, the strain γ_{rz} or γ_{xz}? This question will not be addressed in this thesis. A second approximation involves the estimation of the γ_{rz} strain as

$$\gamma_{rz} = \frac{\Delta u}{\Delta z}$$

whereas in fact

$$\gamma_{rz} = \frac{\partial u}{\partial z} + \frac{\partial w}{\partial r}$$

and the second term will not be zero in these tests. Once again the error committed by this approximation will not be assessed in this work. The two approximations whose degree of accuracy will be checked here are:

1. The determination of the strain from the difference between the displacements at two different depths, representing an average strain over that depth and therefore an assumption of a constant strain between measurement points. The situation is even worse if one considers only the difference between maximum displacement amplitudes rather than the maximum of the amplitude difference over time (which requires the computation of Δu as a function of time).
2. The determination of the shear wave velocity from the time lag between the maximum displacements implying a constant velocity of propagation whereas in fact the level of shear strain and thus the wave propagation velocity vary with time.

In this work we use a cone model to assess the importance of some of the simplifying assumptions introduced in the interpretation of the data from the dynamic tests on a circular slab. The main points to be studied are the calculation of the strains

from the maximum displacements measured at the receivers and the determination of the shear wave velocity from the times of occurrence of the peak displacements (implying a constant, or average, velocity of propagation with time while the properties of the material are changing).

The analytical formulation and two discrete models, one based on the use of springs and lumped masses, the other using finite differences are described in Section 2. The resulting strains at various depths for the two models and different values of the distance between masses (length of the springs) in the first case, and the mesh size in the second, are compared to the analytical results. On the basis of these comparisons it was decided to use the springs and masses model with two different spring lengths for the nonlinear studies. A distance between masses of 0.10 m was used because this is approximately the distance between the receivers in the field tests. A distance of 0.05 m was also used, for comparison, because it provided a slightly better agreement with the analytical solution. The finite difference using second-order central difference model on the other hand required a mesh size of 0.01 m to get reasonable results. For this mesh size the strains were in very good agreement with the analytical results (similar to that of the springs model with 0.05 m separation) but the displacement at the top had still a larger difference.

The results of the nonlinear analyses and the evaluation of the accuracy of the procedure used in practice to obtain the values of $\frac{G}{G_{MAX}}$ versus γ from the measurements are presented in Section 3. Comparisons are made between the curves computed directly

in the computer program from the maximum shear strain and the corresponding value of the shear modulus for each spring and the values obtained from the determination of the shear wave velocity using the difference between the times at which the peak displacements occur at the various receivers. The results are also compared to those obtained computing the shear strain from the difference between the maximum displacements.

Summary and Conclusions are presented in Section 5 along with recommendations for future work.

2. FORMULATION

2.1 Introduction

For the linear elastic case Meek and Veletsos (1974) had pointed out that a cone could represent exactly the stiffness (both real and imaginary parts or spring and dashpot) of a circular foundation on the surface of an elastic half space. This concept was further developed by Wolf, who in 2004 published a book on the subject (Wolf and Deeks) presenting cone solutions for a number of different excitations and layered soils where the properties vary with depth. In this case, however, a new cone is generated at each interface and this ‘simplified’ procedure becomes in fact more cumbersome and complicated than a finite element solution with an absorbing boundary (Kausel, 1974). It should be pointed out, in addition, that although a shear cone, with only shear deformations, will provide the correct values for the horizontal stiffness of a circular mat, it will not reproduce exactly the state of strains and stresses in the soil since in the real problem a horizontal force will produce both a horizontal displacement and a small rotation of the foundation, with a fully three dimensional state of stresses.

In this work we use the cone model to assess the importance of some of the simplifying assumptions introduced in the interpretation of the data from the dynamic tests on a circular slab. The main points to be studied are the calculation of the strains from the maximum displacements of the receivers and the determination of the shear wave velocity from the times of occurrence of the peak displacements (implying a

constant, or average, velocity of propagation with time while the properties of the material are changing). For this purpose the fact that the cone model does not reproduce the true conditions of the tests (more so when considering a single cone while the properties vary with depth due to the nonlinear soil behavior) does not seem important and it is more interesting than the use of a shear beam with constant cross section, since the strains will vary with depth.

The cone will be reproduced with two different discrete models: a series of lumped masses and interconnecting springs, and a finite difference using second-order central difference formulation. In both cases the solution in the linear elastic range should converge to the theoretical solution as the distance between the masses in the first case and the mesh size in the second tend to zero. The formulation of the cone and the two discrete models is presented in this section. The computer programs developed implementing the two discrete models are then validated comparing their results to the analytical predictions for the cone.

2.2 Analytical Formulation

Calling G the shear modulus, c the shear wave velocity and ρ the mass density of the soil and ν Poisson's ratio

$$G = \rho c^2$$

For a circular foundation of radius r_o on the surface of an elastic half space, the horizontal stiffness at a frequency Ω is (Luco and Westman 1971, Veletsos and Wei 1971, Veletsos and Verbic 1974, Kausel 1974)

$$k = (\frac{8Gr_o}{2-\nu})(k_1 + \frac{i\Omega r_o c_1}{c})$$

where k_1 is approximately 1 and c_1 varies between 0.65 and 0.60 for a Poisson's ratio between 0.3 and 0.5. For ν=0.4 we can write approximately

$$k = 5Gr_o(1 + 0.625\frac{i\Omega r_o}{c})$$

and the amplitude of the horizontal displacement due to a unit force would be

$$|u| = \frac{1}{5G\mathrm{r_o}\sqrt{(1)^2 + (0.625\frac{\Omega \mathrm{r_o}}{c})^2}}$$

For a shear cone with the vertex at an elevation z_o above the free surface of the soil and a radius r_o at the free surface, calling z the depth or distance, from the vertex one would have

Radius $$r = r_o \frac{z}{z_o}$$

Area $$A = A_o \frac{z^2}{z_o^2} = \pi r_o^2 \frac{z^2}{z_o^2}$$

Displacement $$u = u_o \frac{z_o}{z} e^{i\frac{\Omega}{c}(ct - z + z_o)}$$

Shear Strain $$\gamma = -\frac{du}{dz} = u_o\left(\frac{z_o}{z^2} + i\frac{\Omega}{c}\frac{z_o}{z}\right)e^{i\frac{\Omega}{c}(ct - z + z_o)}$$

if the *z*-axis points down.

The applied force at the surface would be

$$P = GA_o\gamma(z_o) = GA_o u_o\left(\frac{1}{z_o} + \frac{i\Omega}{c}\right)$$

giving a stiffness

$$k = \frac{\pi r_o G}{z_o}\left(1 + \frac{i\Omega z_o}{c}\right)$$

Comparing this expression with the theoretical one, to get the same result one should have

$$\frac{\pi r_o^2 G}{z_o} = \frac{8Gr_o}{2-\nu}$$

$$\frac{\pi r_o^2 G}{z_o}\frac{\Omega z_o}{c} = \frac{8Gr_o}{2-\nu}\frac{\Omega r_o}{c}c_1$$

leading to

$$\frac{r_o}{z_o} = \frac{8}{\pi(2-\nu)} \text{ or } z_o = \frac{\pi r_o}{8}(2-\nu)$$

Thus the cone's opening angle (or height of the vertex above the free surface of the soil.), would be only affected by Poisson's ratio,

and $$\frac{\Omega z_o}{c} = \frac{\Omega r_o}{c} c_1$$

or $$c_1 = \frac{z_o}{r_o} = \frac{\pi}{8}(2-\nu)$$

For ν =0.4 the elevation of the vertex of the cone above the free surface should be

$$z_o = 0.2\pi r_o = 0.628 r_{o.}$$

And this would result in a coefficient c_1=0.628

Using then a cone with this z_o

$$|u_o| = \frac{P}{5Gr_o} \frac{1}{\sqrt{1+(0.628\frac{\Omega r_o}{c})^2}}$$

$$|u| = \frac{P}{5Gr_o} \frac{z_o}{z} \frac{1}{\sqrt{1+(0.628\frac{\Omega r_o}{c})^2}}$$

and $$|\gamma| = \frac{P}{5Gr_o} \frac{z_o}{z^2} \frac{\sqrt{1+(\frac{\Omega z}{c})^2}}{\sqrt{1+(0.628\frac{\Omega r_o}{c})^2}}$$

2.3 Spring and Mass Model

Considering a truncated cone with height Δz between the depths $z_{i-1} = z_o + (i-1)\Delta z$ and $z_i = z_o + i\Delta z$

$$-GAu' = -GA_o u_o' = P$$
$$u' = -\frac{P}{GA} = -\frac{Pz_o^2}{A_o G z^2}$$

Then if u =0 at z=z_i

$$u(z_{i-1}) = \frac{Pz_o^2}{A_O G}\left(\frac{1}{z_{i-1}} - \frac{1}{z_i}\right) = \frac{Pz_o^2}{A_O G}\frac{\Delta z}{z_i z_{i-1}}$$

and the corresponding spring stiffness would be

$$k_i = \frac{A_o G}{\Delta z}\frac{z_{i-1}z_i}{z_o^2}$$

representing an equivalent area

$$A_{eq} = \pi r_o^2 \frac{z_{i-1}z_i}{z_o^2}$$

The volume of the truncated cone is

$$V = \frac{\pi r_o^2}{3z_o^2}(z_i^3 - z_{i-1}^3) = \frac{\pi}{3} r_o^2 \Delta z \frac{z_i^2 + z_i z_{i-1} + z^2{}_{i-1}}{z_o^2}$$

and the total mass would be

$$M = \frac{\pi}{3}\rho r_o^2 \Delta z \frac{z_i^2 + z_i z_{i-1} + z_{i-1}^2}{z_o^2}$$

Half of this mass would be lumped at each end of the ith spring.

2.4 Finite Difference Using Second-Order Central Difference Model

The equation of motion for the cone is

$$\frac{d}{dz}(GAu') = GAu'' + (GA)'u' = pA\ddot{u}$$

with boundary condition at $z=z_o$

$$(GA)_o u_o' = -P$$

and initial conditions

$$u(z,0) = 0$$
$$\dot{u}(z,0) = 0$$

Using finite differences using second-order central difference with a mesh size Δz

and

$$u_i'' = \frac{u_{i+1} - 2u_i + u_{i-1}}{\Delta z^2}$$
$$u_i' = \frac{u_{i+1} - u_{i-1}}{2\Delta z}$$

leading to the discrete equation of motion at point i and time t

$$\rho A_i \ddot{u}_i = (GA)_i \frac{u_{i+1} - 2u_i + u_{i-1}}{\Delta z^2} + \frac{(GA)_{i+1} - (GA)_{i-1}}{2\Delta z} \frac{u_{i+1} - u_{i-1}}{2\Delta z}$$

and discretizing in time

$$u_{i,n+1} = 2u_{i,n} - u_{i,n-1} + \frac{\Delta t^2}{\rho A_i}\left[(GA)_i \frac{u_{i+1} - 2u_i + u_{i-1}}{\Delta z^2} + \frac{(GA)_{i+1} - (GA)_{i-1}}{2\Delta z} \frac{u_{i+1} - u_{i-1}}{2\Delta z} \right]_n$$

where the second subscript n denotes time $n\Delta t$.

Initially

$$u_{t,o} = 0$$

$$u_{i,1} = 0 \qquad \text{if the load is of the form } P\sin(\Omega t)$$

at the top point

$$GA_o \frac{u_1 - u_{-1}}{2\Delta z} = -P$$

$$u_{-1} = u_1 + 2P\Delta z$$

and $$u_i - 2u_o + u_{-1} = 2(u_1 - u_o) + 2P\Delta z$$

Finally $$(GA)_{-1} = -3(GA)_o + 4(GA)_1 - (GA)_2$$

thus at the top point the equation becomes

$$u_{o,n+1} = 2u_{o,n} - u_{o,n-1} + \frac{\Delta t^2}{\rho A_o}\left[(GA)_o \frac{2(u_1 - u_o) + 2P\Delta z}{\Delta z^2} - \frac{P}{(GA)_o}\frac{(GA)_1 - (GA)_{-1}}{2\Delta z}\right]_n$$

with $P_n = P\sin(\Omega t_n) = P\sin(n\Omega\Delta t)$

For both models the bottom was placed at a sufficient distance to guarantee that reflections would not arrive at the top part during the time range of interest and the time increment Δt was taken small enough to guarantee stability of the integration. (Figure 2.1)

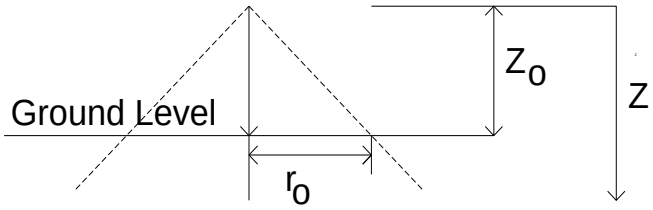

Figure 2.1 Cone Model

2.5 Validation of the Discrete Models

2.5.1 Displacements

Program TOR1 implemented the model with lumped masses and springs and program TOR2 implemented the finite difference using second-order central difference formulation. Both programs were run with different mesh sizes, or length of the springs in the first case, in order to study the convergence of the results to the analytical solution. Frequencies of 10, 50 and 100 Hz were considered.

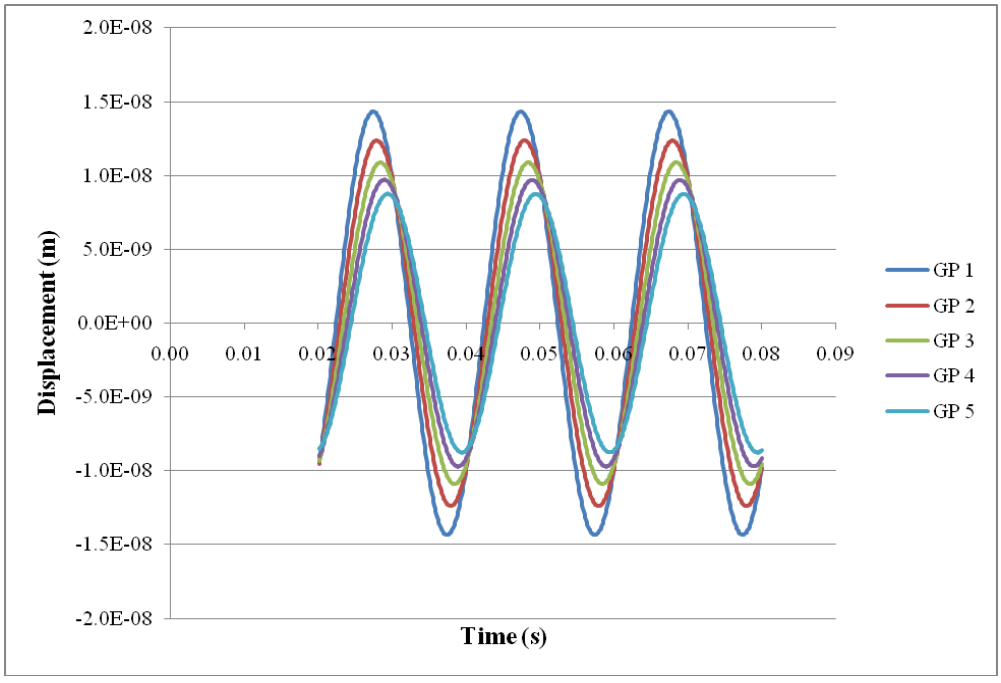

Figure 2.2 Displacement History--TOR 1 with Δz= 0.05 m f=50 Hz

Table 2.1 Maximum Values for TOR 1 at different depths

TOR1	t (s)	d (m)	vel (m/s)
Δz=0.05 m f=50 Hz	2.74E-02	1.43E-08	
	2.79E-02	1.24E-08	100
	2.84E-02	1.09E-08	100
	2.89E-02	9.71E-09	100
	2.94E-02	8.77E-09	100
Δz=0.10 m f=50 Hz	2.75E-02	1.47E-08	
	2.85E-02	1.11E-08	100
	2.95E-02	8.97E-09	100
	3.05E-02	7.53E-09	100
	3.15E-02	6.49E-09	100
Δz=0.2 m f=50 Hz	2.77E-02	1.62E-08	
	2.98E-02	1.00E-08	95.24
	3.19E-02	7.26E-09	95.24
	3.40E-02	5.67E-09	95.24
	3.61E-02	4.63E-09	95.24

For the springs model (TOR1) mesh sizes of 0.05, 0.10 and 0.20 m were considered. The displacement time histories at the surface and at depths for Δz= 0.10 m

for all cases are shown in Figure 2.2 for a frequency of 50 Hz. The maximum values are listed in Table 2.1.

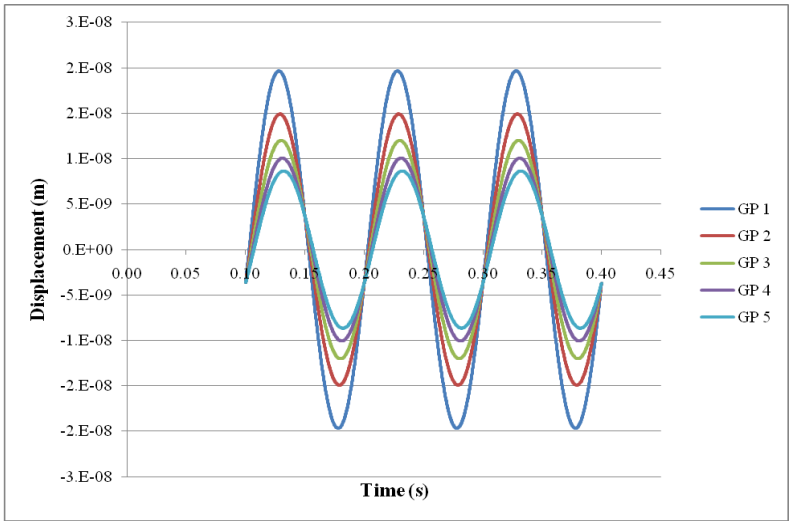

Figure 2.3 Displacement History--TOR 1 with Δz= 0.10 m f=10 Hz

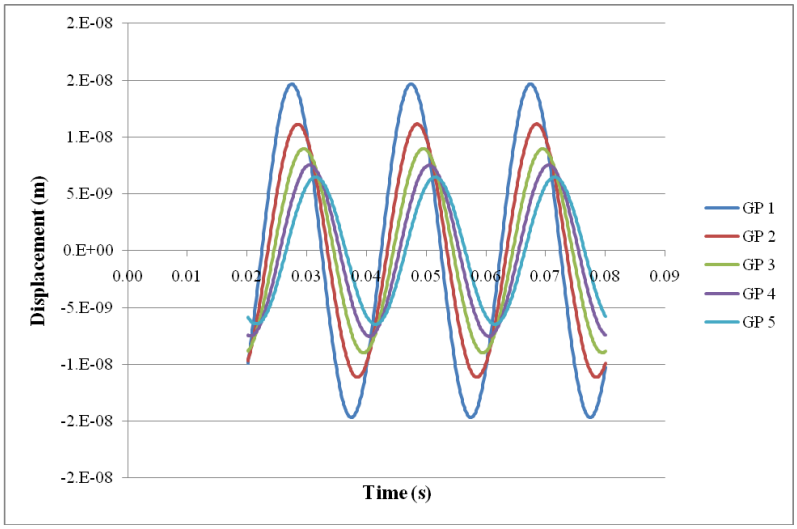

Figure 2.4 Displacement History--TOR 1 with Δz= 0.10 m f= 50 Hz

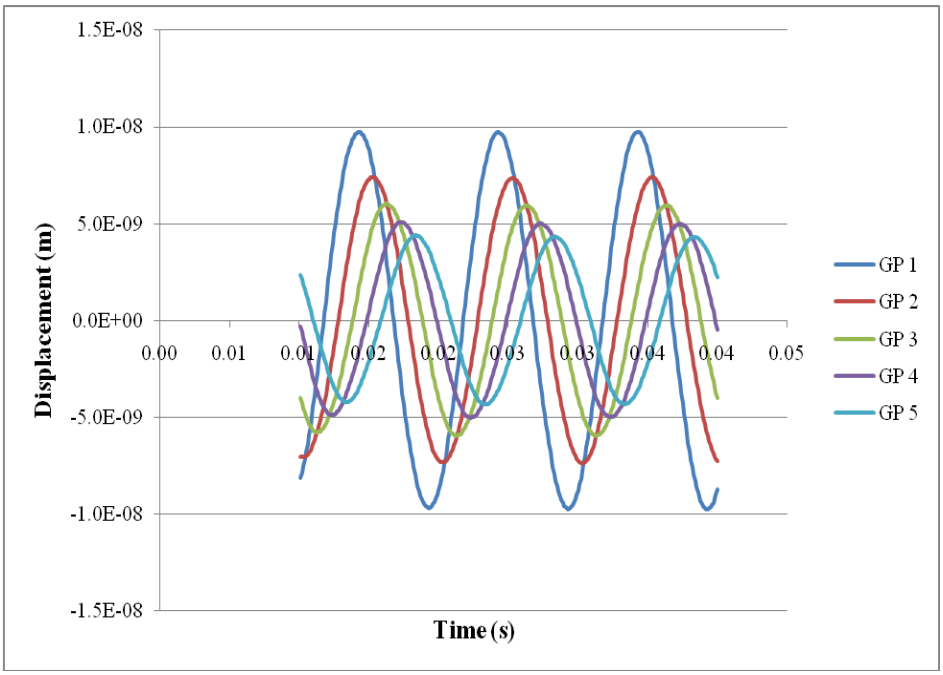

Figure 2.5 Displacement History--TOR 1 with Δz= 0.10 m f= 100 Hz

In all cases, it can be seen that there is a clear shift in time between the occurrence of the peak values at the different depths. The resulting propagations velocities computed from the times of occurrence of the maxima and the distance between points are also listed in Table 2.1. Figures 2.3 to 2.5 shows the displacement time histories for Δz of 0.10 m and frequencies of 10, 50 and 100 Hz.

Mesh sizes of 0.10, 0.05 and 0.01 m were considered for the finite difference using the second-order central difference formulas (program TOR2). It should be noticed that in order to get accurate results the mesh size for the finite differences using the second-order central difference formulas had to be much smaller than the Δz used with the lumped masses and springs.

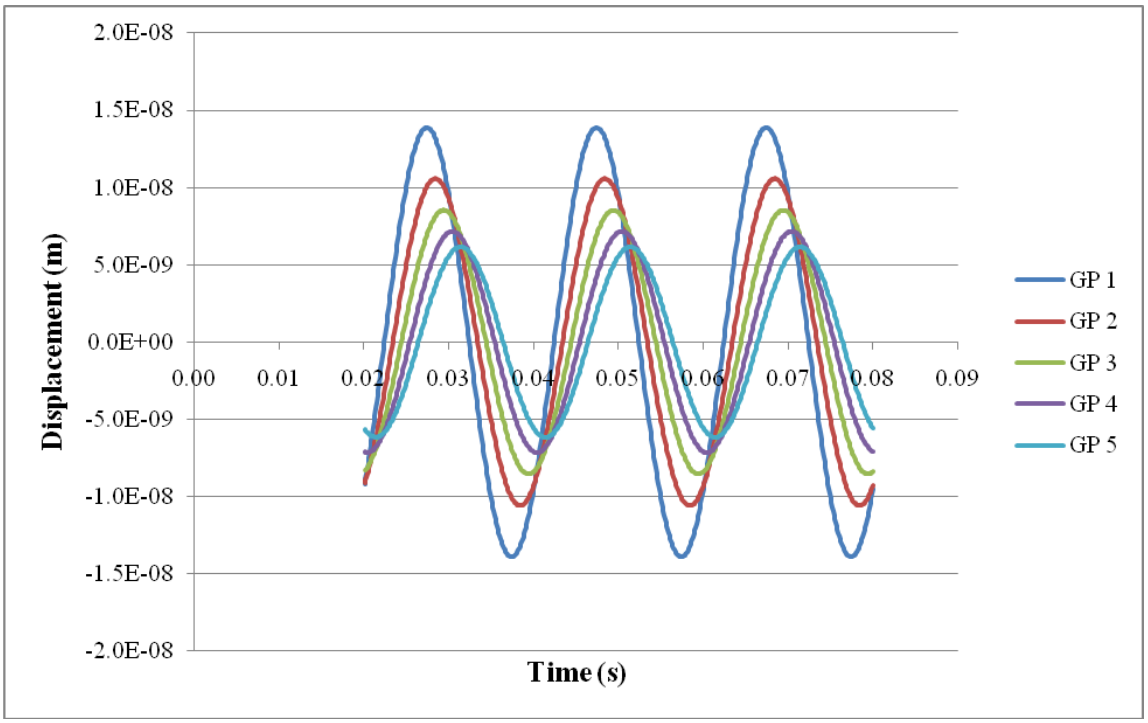

Figure 2.6 Displacement History--TOR 2 with Δz= 0.01 m f= 50 Hz

Table 2.2 Maximum Values for TOR2 at different depths

TOR 2	t (s)	d (m)	v (m/s)
Δz=0.01 m f=50 Hz	2.75E-02	1.39E-08	
	2.84E-02	1.06E-08	100
	2.94E-02	8.54E-09	100
	3.04E-02	7.16E-09	100
	3.14E-02	6.16E-09	100
Δz=0.05 m f=50 Hz	2.75E-02	1.25E-08	
	3.25E-02	5.05E-09	100
	3.75E-02	3.17E-09	100
	4.25E-02	2.31E-09	100
	4.75E-02	1.81E-09	100
Δz=0.10 m f=50 Hz	2.76E-02	1.09E-08	
	3.77E-02	2.88E-09	99
	4.78E-02	1.66E-09	99
	5.78E-02	1.17E-09	100
	6.79E-02	8.98E-10	99

Figure 2.6 shows the displacement time histories at the same depths obtained with TOR2 for a frequency of 50 Hz and the maximum values and computed propagation velocities are listed in Table 2.2.

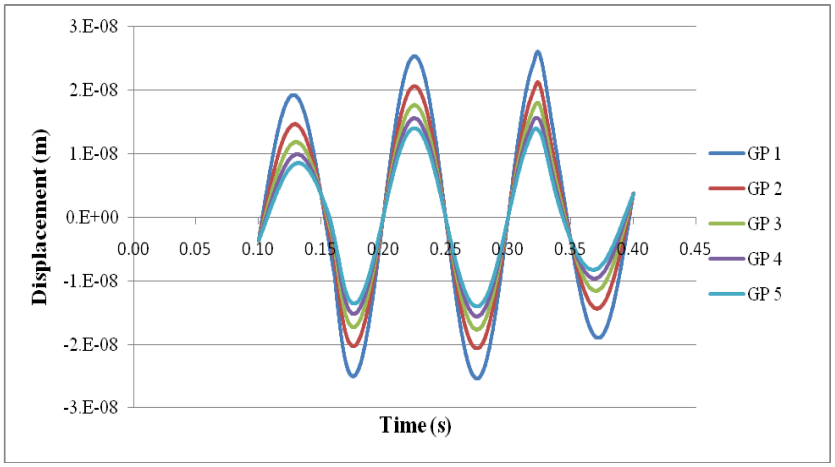

Figure 2.7 Displacement History--TOR 2 with Δz= 0.01 m f=10 Hz

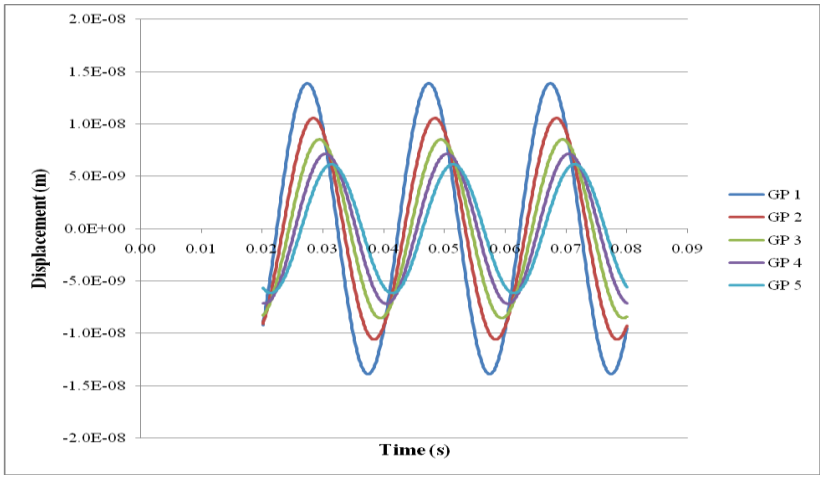

Figure 2.8 Displacement History--TOR 2 with Δz= 0.01 m f=50 Hz

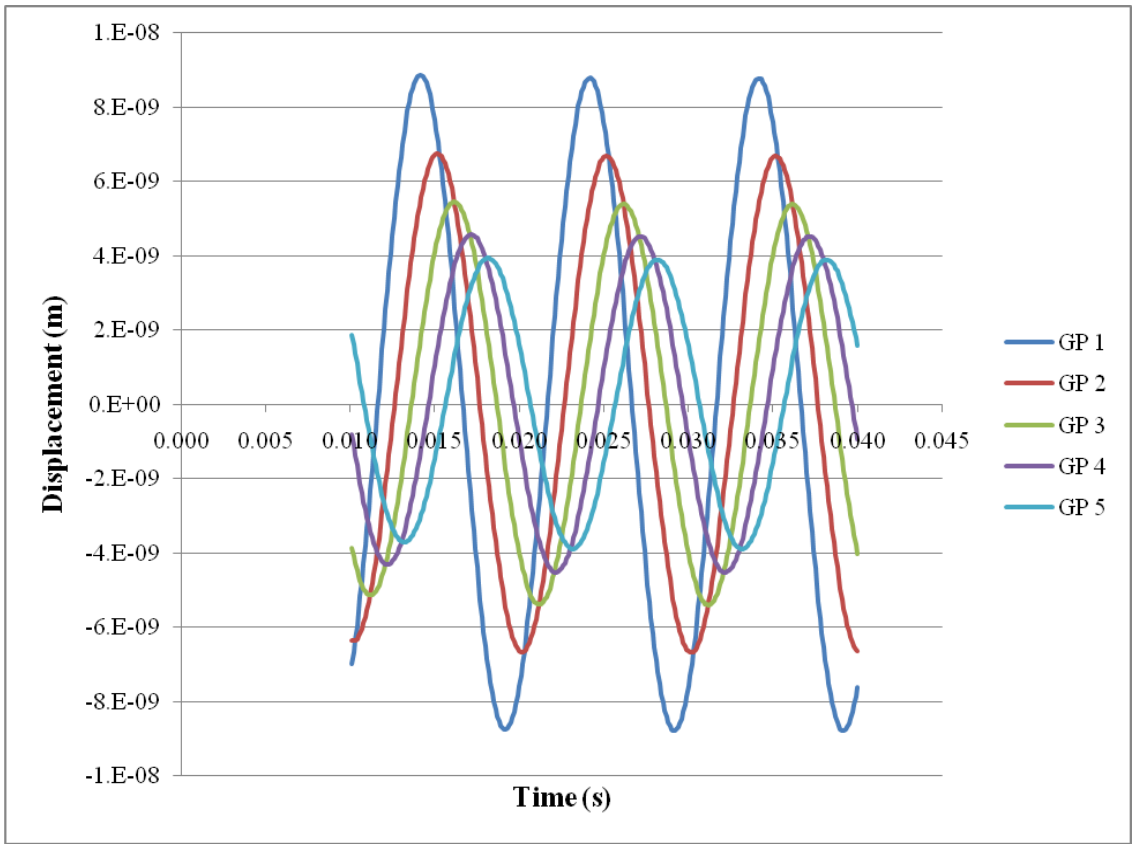

Figure 2.9 Displacement History--TOR 2 with Δz= 0.01 m f= 100 Hz

Figures 2.7 to 2.9 compare the results with TOR2 and a mesh size of 0.01 m for the three frequencies.

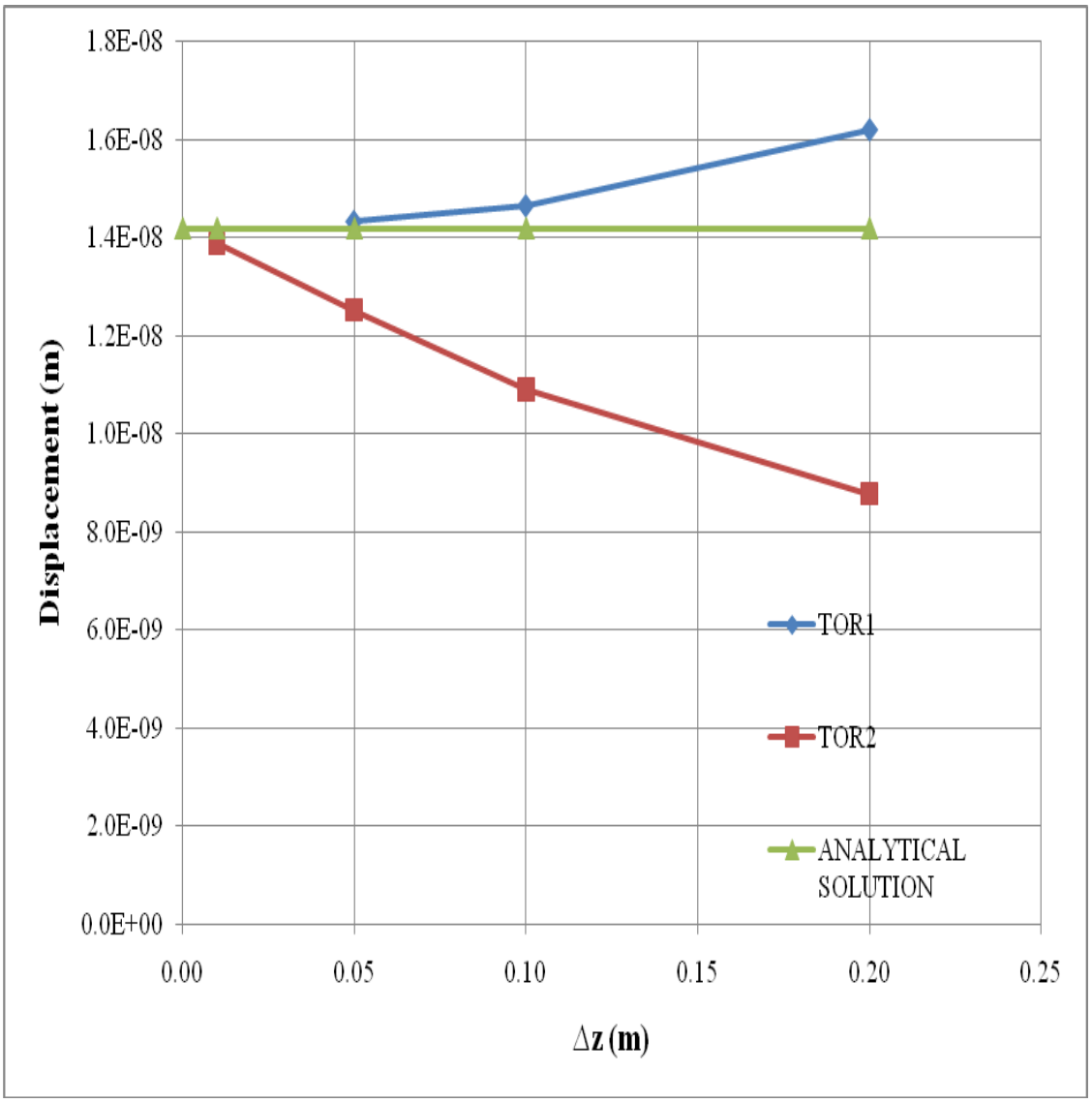

Figure 2.10 Comparison TOR 1 and TOR 2 with analytical solution as a function of Δz

Table 2.3 Results for TOR1, TOR2 and Analytical Solution

	Δz (m)	Disp (m)
TOR1	5.00E-02	1.43E-08
	1.00E-01	1.47E-08
	2.00E-01	1.62E-08
TOR2	1.00E-02	1.39E-08
	5.00E-02	1.25E-08
	1.00E-01	1.09E-08
	2.00E-01	8.78E-09
ANALY		1.42E-08

Figure 2.10 shows the convergence of the value of the displacement at the top with Δz for the 2 models. Table 2.3 lists the results.

2.5.2 Strains

The values of the strains computed with the 3 models and from the analytical formula are compared next. Table 2.4 and Figure 2.11 show the results for TOR1 with Δz=0.10 m and Δz=0.05 m and for TOR2 with Δz=0.01 m. When using a Δz=0.05 m for TOR1 the strains are obtained at twice the number of points and different depths from those with Δz=0.1 m

Figure 2.11 shows that results for TOR1 with Δz=0.05 m and TOR2 with Δz=0.01 m are closer to the analytical curve, whereas the results with TOR1 with Δz=0.10 m are slightly below and to the right of the analytical solution.

Table 2.4 Strains Values for TOR1, TOR2 and ANALY

z (m)	ANALY (m/m)	TOR1 Δz=0.10 m (m/m)	TOR1 Δz=0.05 m (m/m)	TOR2 Δz=0.01 m (m/m)
0	6.37E-08			6.17E-08
0.025			5.799E-08	
0.05	5.12E-08	5.41E-08		
0.075			4.771E-08	
0.1	4.28E-08			4.18E-08
0.125			4.022E-08	
0.15	3.66E-08	3.89E-08		
0.175			3.492E-08	
0.2	3.21E-08			3.16E-08
0.225			3.102E-08	
0.25	2.86E-08	3.03E-08		
0.275			2.784E-08	
0.3	2.58E-08			2.54E-08
0.325			2.513E-08	
0.35	2.35E-08	2.46E-08		
0.375			2.288E-08	
0.4	2.15E-08			2.13E-08
0.425			2.111E-08	
0.45	1.99E-08	2.10E-08		

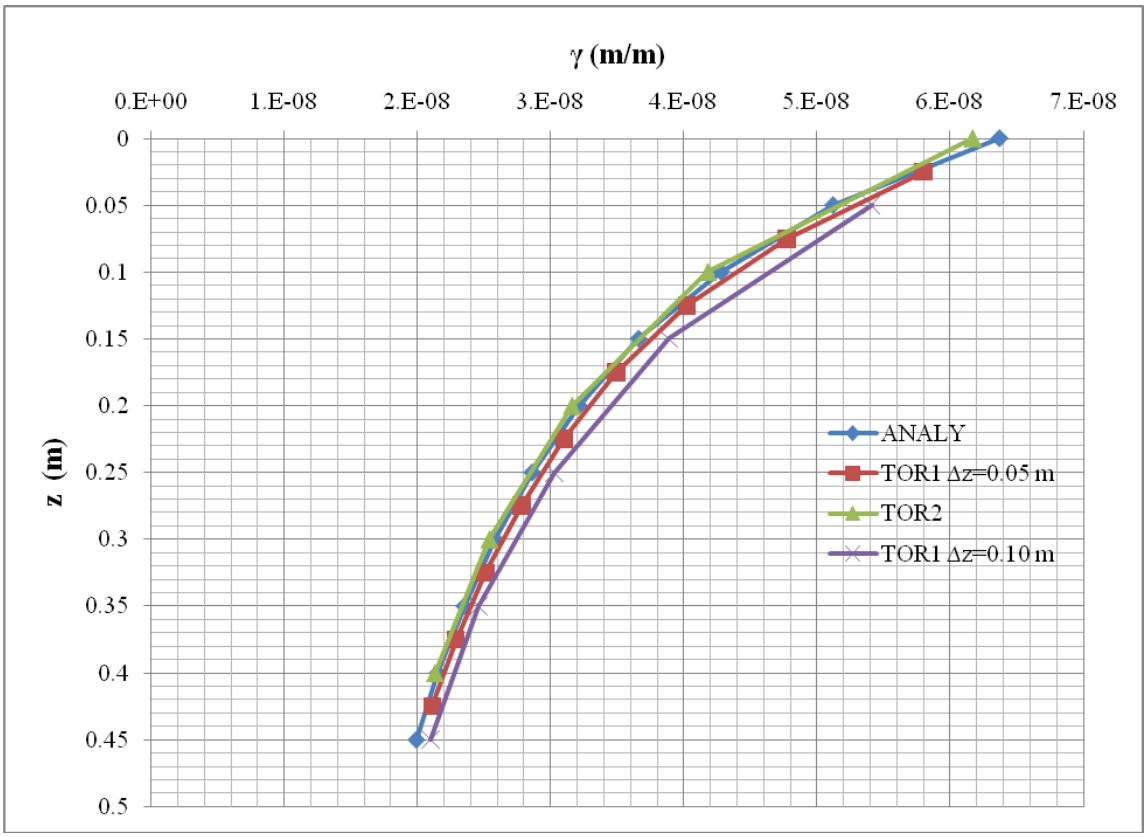

Figure 2.11 Comparison of Strains for TOR 1 with Δz=0.10 m and 0.05 m, TOR2 with Δz=0.01 m and ANALY

3. NONLINEAR ANALYSIS

3.1 Soil Model

The soil properties used were based on actual laboratory data obtained at the University of Texas at Austin (Darendeli, 2001) (Figure 3.1).

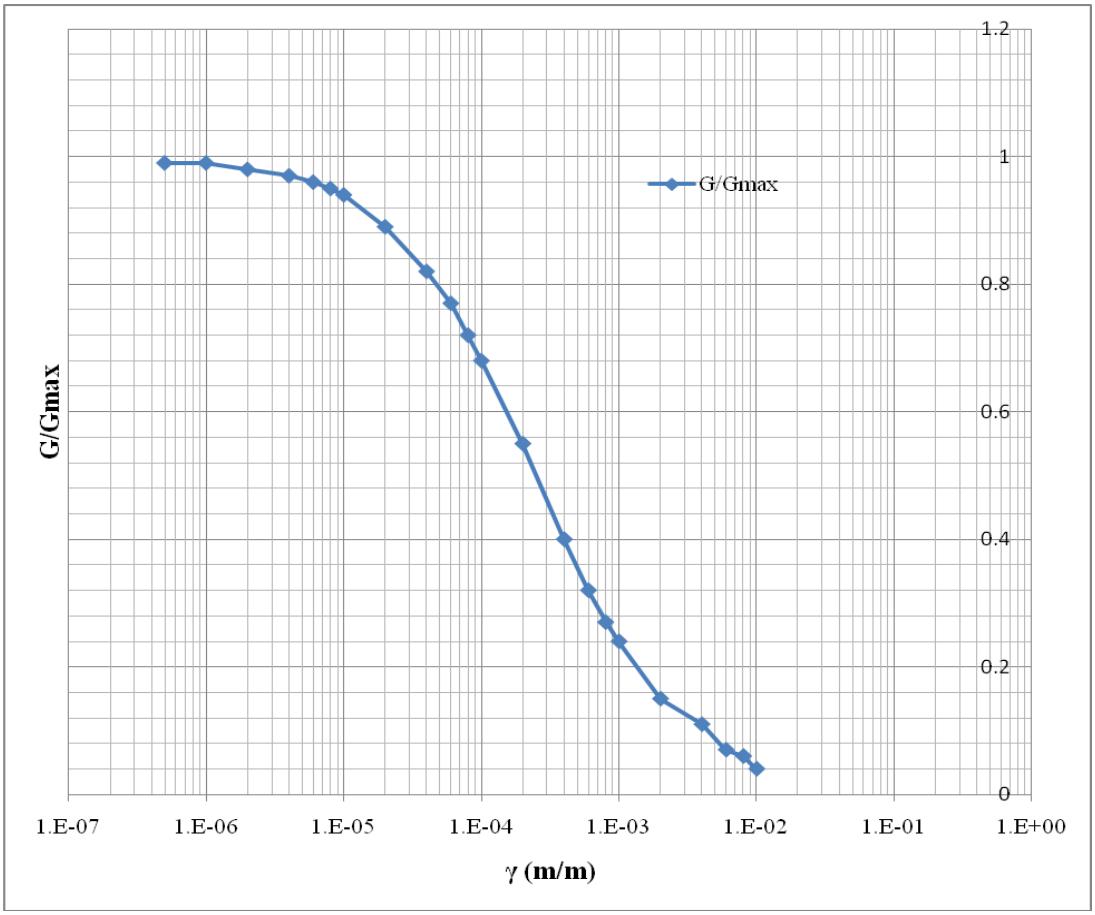

Figure 3.1 $\frac{G}{G_{MAX}}$ vs. γ for springs selected

Table 3.1 $\frac{\tau}{G_{\max}} vs. \gamma$ for springs selected

γ (m/m)	τ/Gmax
5.000E-07	4.950E-07
1.000E-06	9.900E-07
2.000E-06	1.960E-06
4.000E-06	3.880E-06
6.000E-06	5.760E-06
8.000E-06	7.600E-06
1.000E-05	9.400E-06
2.000E-05	1.780E-05
4.000E-05	3.280E-05
6.000E-05	4.620E-05
8.000E-05	5.760E-05
1.000E-04	6.800E-05
2.000E-04	1.100E-04
4.000E-04	1.600E-04
6.000E-04	1.920E-04
8.000E-04	2.160E-04
1.000E-03	2.400E-04
2.000E-03	3.000E-04
4.000E-03	4.400E-04
6.000E-03	4.200E-04
8.000E-03	4.800E-04
1.000E-02	4.000E-04

From these values a series of nonlinear elasto-plastic springs in parallel that would reproduce at least approximately the behavior were obtained using a procedure suggested by Iwan (1967). For a given value of the strain the total force (stress) would be the sum of the forces in all the springs. Each spring is then characterized by an initial modulus $\bar{G}_i$ and a yield strain γ_{yi} with τ_y a yield stress $\tau_{yi} = \bar{G}_i \gamma_{yi}$. Given n points in the curve of G vs. γ we would have

$$\bar{G}_n = \frac{\tau_n - \tau_{n-1}}{\gamma_n - \gamma_{n-1}} \text{ or } \frac{G_n\gamma_n - G_{n-1}\gamma_{n-1}}{\gamma_n - \gamma_{n-1}} \qquad \gamma_{yn} = \gamma_n$$

and

$$\bar{G}_i = \frac{G_i\gamma_i - G_{i-1}\gamma_{i-1}}{\gamma_i - \gamma_{i-1}} + \sum_{j=i+1}^{n} k_j \text{ or } \frac{z_i - z_{i-1}}{\gamma_i - \gamma_{i-1}} + \sum_{j=i+1}^{n} k_j \qquad \gamma_{yi} = \gamma_i$$

$$\text{where } G_o = G_{\max} \text{ and } \gamma_o = 0$$

The corresponding $\frac{\tau}{G_{\max}}$ vs. γ is shown in Figure 3.2 and the variation of $\frac{G}{G_{\max}}$ vs. γ in Figure 3.3. The values of $\frac{\tau}{G_{\max}} vs. \gamma$ are listed in Table 3.1.

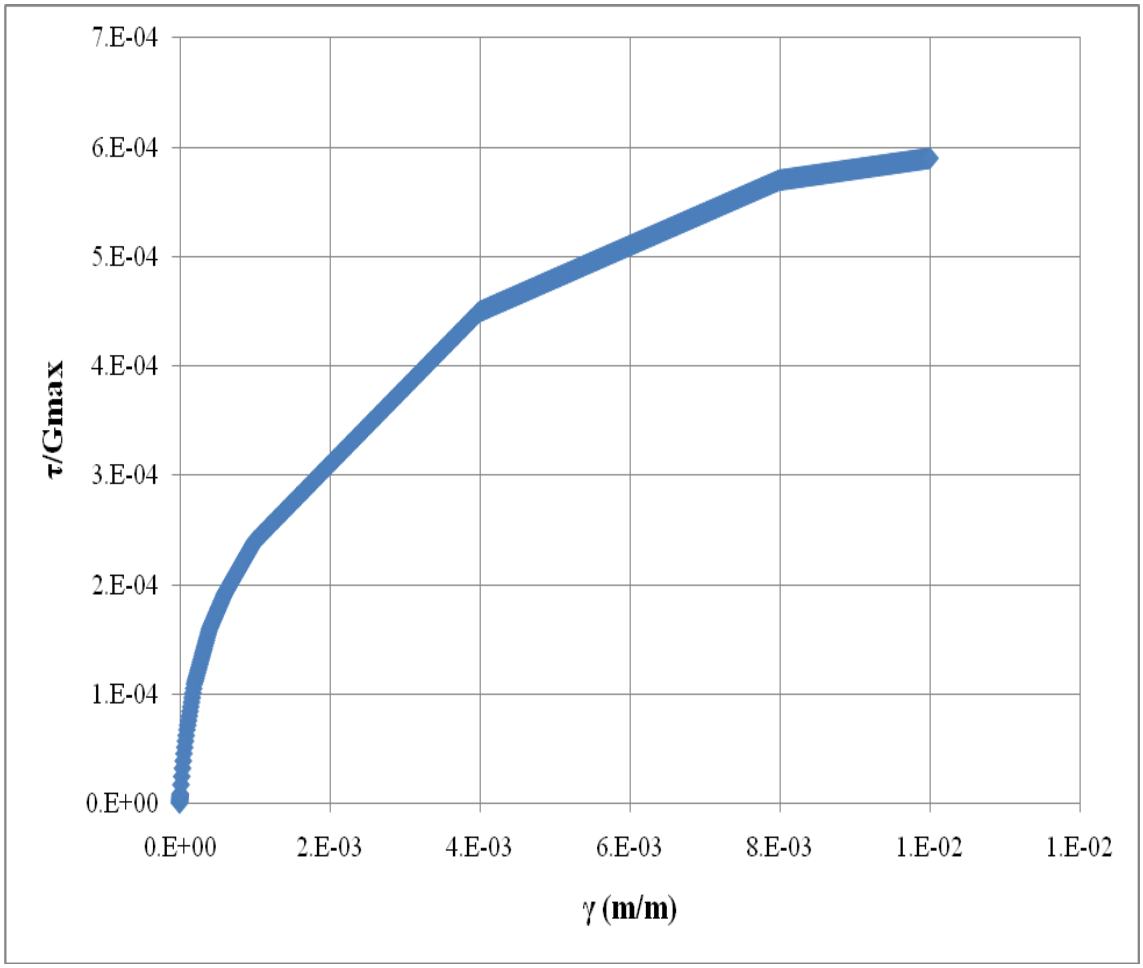

Figure 3.2 $\frac{\tau}{G_{max}} vs. \gamma$ for springs selected

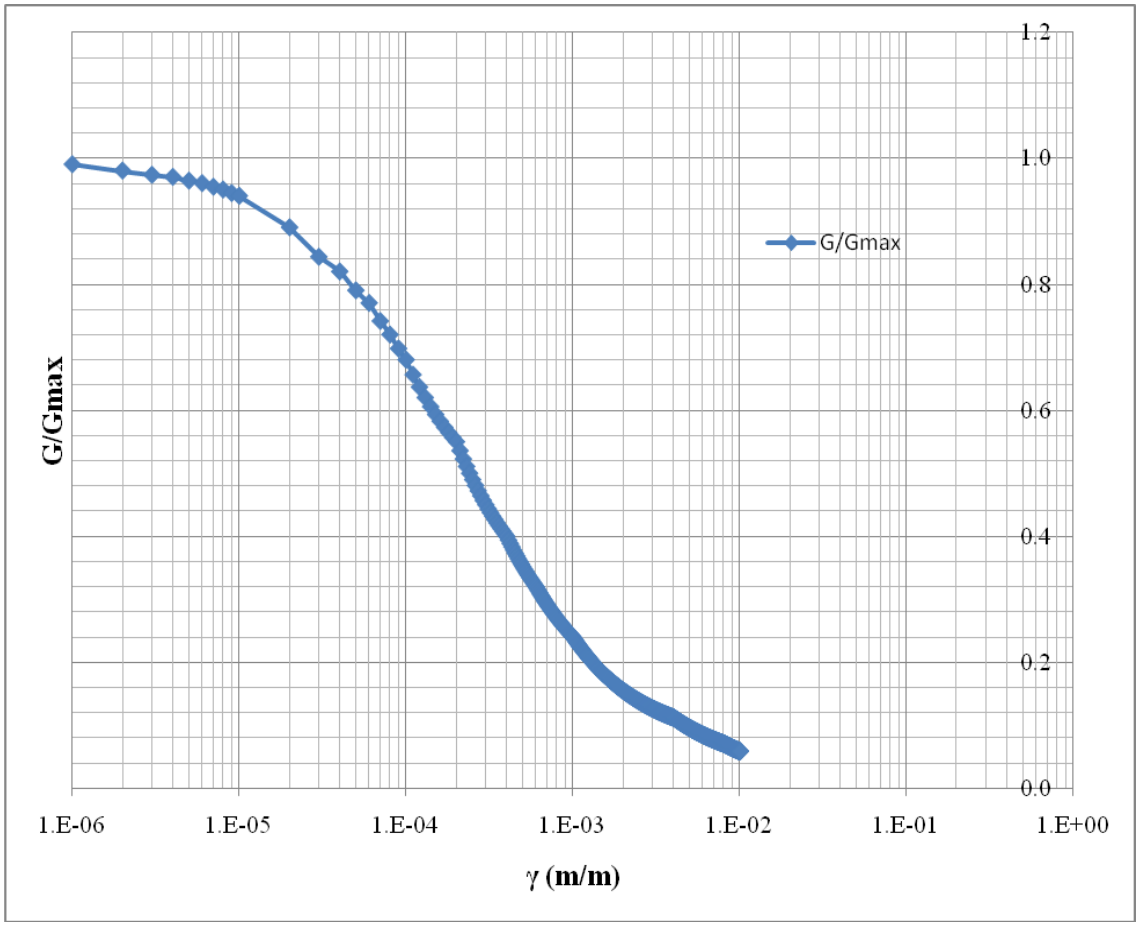

Figure 3.3 $\frac{G}{G_{MAX}}$ vs. γ for springs selected

The values of k_i and γ_{yi} defined the nonlinear springs in parallel used to reproduce the nonlinear characteristics of each spring in the discrete mass and springs model and the values of G at each point in the finite difference model.

3.2 Procedure

Runs were performed with programs TOR1with Δz=0.10 m and Δz=0.05 m. The value of Δz=0.10 m was used because that is approximately the distance between receivers in the field tests. The value of Δz=0.05 m was used because it provided more accurate results in the linear range and as a measure of comparison. TOR2 required a much smaller Δz and its displacements were not as accurate as those obtained with TOR1 and Δz=0.05 m so it was not used for the nonlinear studies. For a soil deposit with an initial (low level of strains) shear wave velocity of 100 m/sec, a mass density of 2000 $\frac{kg}{m^3}$ and therefore a maximum shear modulus $G_{\max}$ of $2X10^7$ Pa, a slab with a radius of 0.5 m was subjected to harmonic forces with a frequency of 50 Hz and varying amplitudes. The harmonic force amplitudes were 100, 500, 1000, 5000, and 10,000 N for Δz=0.10 m. Harmonic force amplitudes for Δz=0.05 m were 100, 500, 1000, and 5000 N because for a depth of 0.025 m the strain corresponding to a force of 10,000 N exceeded the maximum strain considered in the $\frac{G}{G_{MAX}}$ curve. The displacements were printed at the surface and depths of 0.10, 0.20, 0.30 and 0.40 m.

In the model with Δz=0.10 m the resulting strains and values of the modulus for each spring would be at depths of 0.05, 0.15, 0.25 and 0.35 m. For Δz=0.05 the depths would be 0.025, 0.075, 0.125, 0.175, 0.225, 0.5 and 0 m. The propagation velocities were then computed from the times between the maximum displacements at the difference depths.

3.3 Results

Tables 3.2 and 3.3 list the results for the two values of Δz. The results tabulated are the γ_{MAX} and $\frac{G}{G_{MAX}}$ obtained directly from the program, the value of $\frac{c}{c_{MAX}}$ squared that should in principle be equal to $\frac{G}{G_{MAX}}$ with the shear wave velocity computed from the difference between the times of occurrence of the peak displacements at two consecutive receivers, and the shear strain $\tilde{\gamma}$ computed as the difference between the maximum displacements of two receivers divided by their distance. Figure 3.4 shows the agreement between the values of $\frac{G}{G_{MAX}}$ versus γ obtained for both cases from the direct computation of $G_{\max}$ and γ_{MAX} and the assumed material curve. As expected the agreement is excellent. This verifies that the correct variation of G with γ is being used in the computer program. Figure 3.5 shows the values of the shear modulus curve from the experimental data (the assumed material properties) along with γ and the $\frac{c}{c_{MAX}}$ results, for Δz=0.01 and 0.05 m (γ is the maximum shear strain computed by the program). It can be seen that the values of $\frac{c^2}{c^2_{MAX}}$ are always larger than those of $\frac{G}{G_{MAX}}$. This indicates that the shear wave velocity computed is an average velocity over time rather than the minimum velocity corresponding to γ_{MAX}.

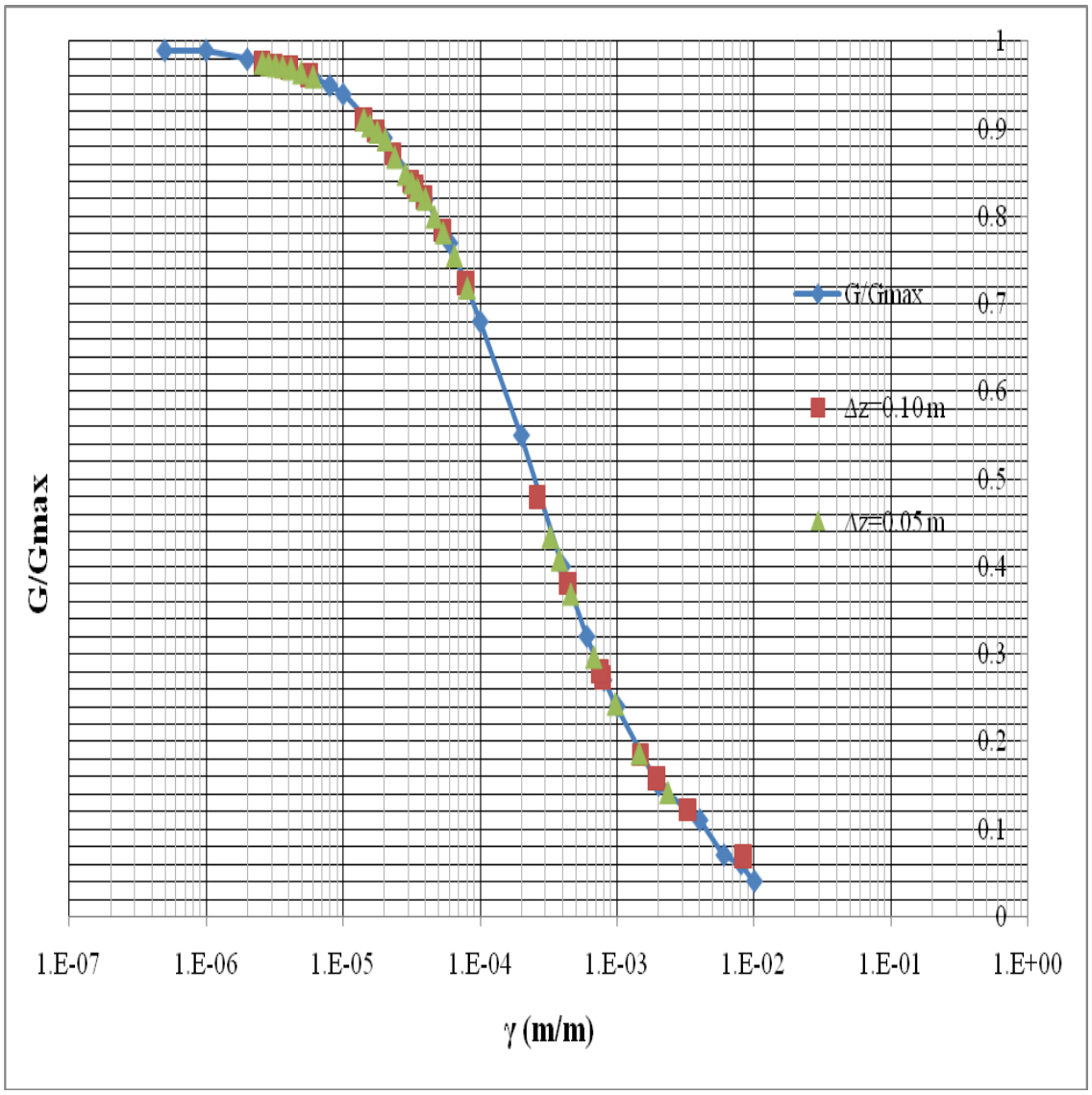

Figure 3.4 Shear Modulus Curve with Δz=0.05 m and 0.10 m.

Figure 3.6 shows the values of the shear modulus curve from the experimental data along with the results of $\frac{G}{G_{MAX}}$ versus $\tilde{\gamma}$ for Δz= 0.1 m and Δz= 0.05 m. It can be seen that the $\tilde{\gamma}$ is always smaller than the actual γ_{MAX} and therefore the results are now to the left of the experimental (assumed) curve.

Figure 3.7 shows the values of the shear modulus curve from the experimental data along with the results of $\frac{c^2}{c^2{}_{MAX}}$ versus $\tilde{\gamma}$ for Δz=0.1 m and 0.05 m. In this case the errors committed using data $\frac{c^2}{c^2{}_{MAX}}$ and $\tilde{\gamma}$ being of opposite sign the agreement is a little better but still the results are to the left indicating that the error committed using the $\tilde{\gamma}$ is larger.

Figures 3.8 to 3.12 show the displacement time histories for Δz of 0.10 m, frequency of 50 Hz and harmonic forces of 100, 500, 1000, 5000, and 10,000 N. The displacements increase and periods elongate as the load increases.

Figures 3.13 to 3.16 show the displacement time histories for Δz of 0.05 m, frequency 50 Hz and harmonic forces of 100, 500, 1000 and 5000 N. The same trends can be observed.

Table 3.2 Values for TOR1 Δz=0.1 m

TOR1 Δz=0.1 m		c (m/s)	γ (m/m)	γ_{max} (m/m)	$\frac{G}{G_{max}}$	$\frac{c^2}{c_{max}^2}$
P=100 N	1	99	1.60E-06	5.63E-06	0.96	0.98
	2	100	1.21E-06	4.05E-06	0.97	1.00
	3	100	9.74E-07	3.12E-06	0.97	1.00
	4	100	8.14E-07	2.55E-06	0.98	1.00
P=500 N	1	93	8.72E-06	3.35E-05	0.83	0.87
	2	94	6.44E-06	2.31E-05	0.87	0.88
	3	95	5.11E-06	1.74E-05	0.90	0.90
	4	97	4.22E-06	1.41E-05	0.91	0.94
P=1,000 N	1	91	1.91E-05	7.81E-05	0.72	0.83
	2	91	1.39E-05	5.27E-05	0.78	0.83
	3	95	1.08E-05	3.89E-05	0.82	0.91
	4	97	8.86E-06	3.12E-05	0.84	0.94
P=5,000 N	1	57	2.95E-04	1.94E-03	0.16	0.33
	2	71	1.46E-04	7.83E-04	0.27	0.51
	3	72	9.19E-05	4.35E-04	0.38	0.53
	4	74	6.61E-05	2.62E-04	0.48	0.54
P=10,000 N	1	34	1.07E-03	8.32E-03	0.07	0.12
	2	47	4.89E-04	3.26E-03	0.12	0.22
	3	58	2.66E-04	1.48E-03	0.18	0.34
	4	66	1.63E-04	7.51E-04	0.28	0.43

Table 3.3 Values for TOR1 Δz=0.05 m

TOR1 Δz=0.05 m		c (m/s)	γ (m/m)	γ_{max} (m/m)	$\frac{G}{G_{max}}$	$\frac{c^2}{c_{max}^2}$
P=100 N	1	96	1.57E-06	6.03E-06	0.96	0.92
	2	98	1.35E-06	4.91E-06	0.96	0.96
	3	98	1.18E-06	4.15E-06	0.97	0.96
	4	99	1.06E-06	3.61E-06	0.97	0.98
	5	100	9.51E-07	3.19E-06	0.97	1.00
	6	100	8.66E-07	2.85E-06	0.97	1.00
	7	100	7.94E-07	2.57E-06	0.98	1.00
P=500 N	1	96	8.56E-06	3.48E-05	0.83	0.92
	2	98	7.26E-06	2.84E-05	0.85	0.96
	3	98	6.30E-06	2.38E-05	0.87	0.96
	4	98	5.57E-06	2.03E-05	0.89	0.96
	5	100	4.99E-06	1.77E-05	0.90	1.00
	6	100	4.52E-06	1.57E-05	0.90	1.00
	7	100	4.13E-06	1.41E-05	0.91	1.00
P=1,000 N	1	88	1.87E-05	8.06E-05	0.72	0.77
	2	93	1.57E-05	6.49E-05	0.76	0.86
	3	94	1.35E-05	5.38E-05	0.78	0.88
	4	94	1.19E-05	4.62E-05	0.80	0.88
	5	96	1.06E-05	3.98E-05	0.82	0.92
	6	100	9.53E-06	3.49E-05	0.83	1.00
	7	100	8.66E-06	3.16E-05	0.84	1.00
P=5,000 N	1	52	2.86E-04	2.35E-03	0.14	0.27
	2	54	1.98E-04	1.45E-03	0.19	0.29
	3	60	1.45E-04	9.72E-04	0.24	0.35
	4	65	1.11E-04	6.78E-04	0.30	0.42
	5	68	8.91E-05	4.59E-04	0.37	0.46
	6	71	7.53E-05	3.79E-04	0.41	0.50
	7	75	6.44E-05	3.25E-04	0.43	0.56

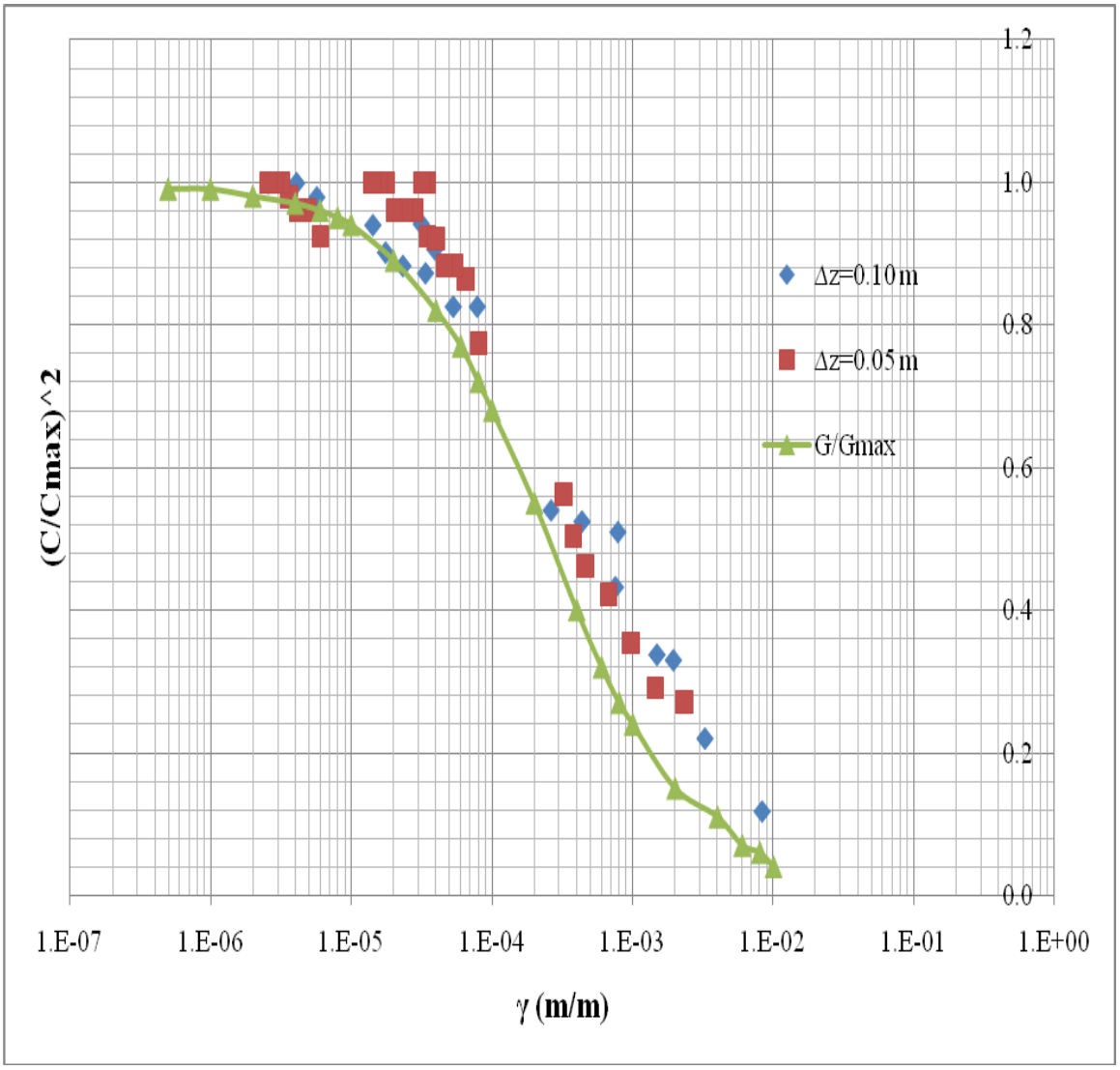

Figure 3.5 Shear Modulus Curve with $\frac{c^2}{c^2_{MAX}}$ for Δz=0.10 m and 0.05 m

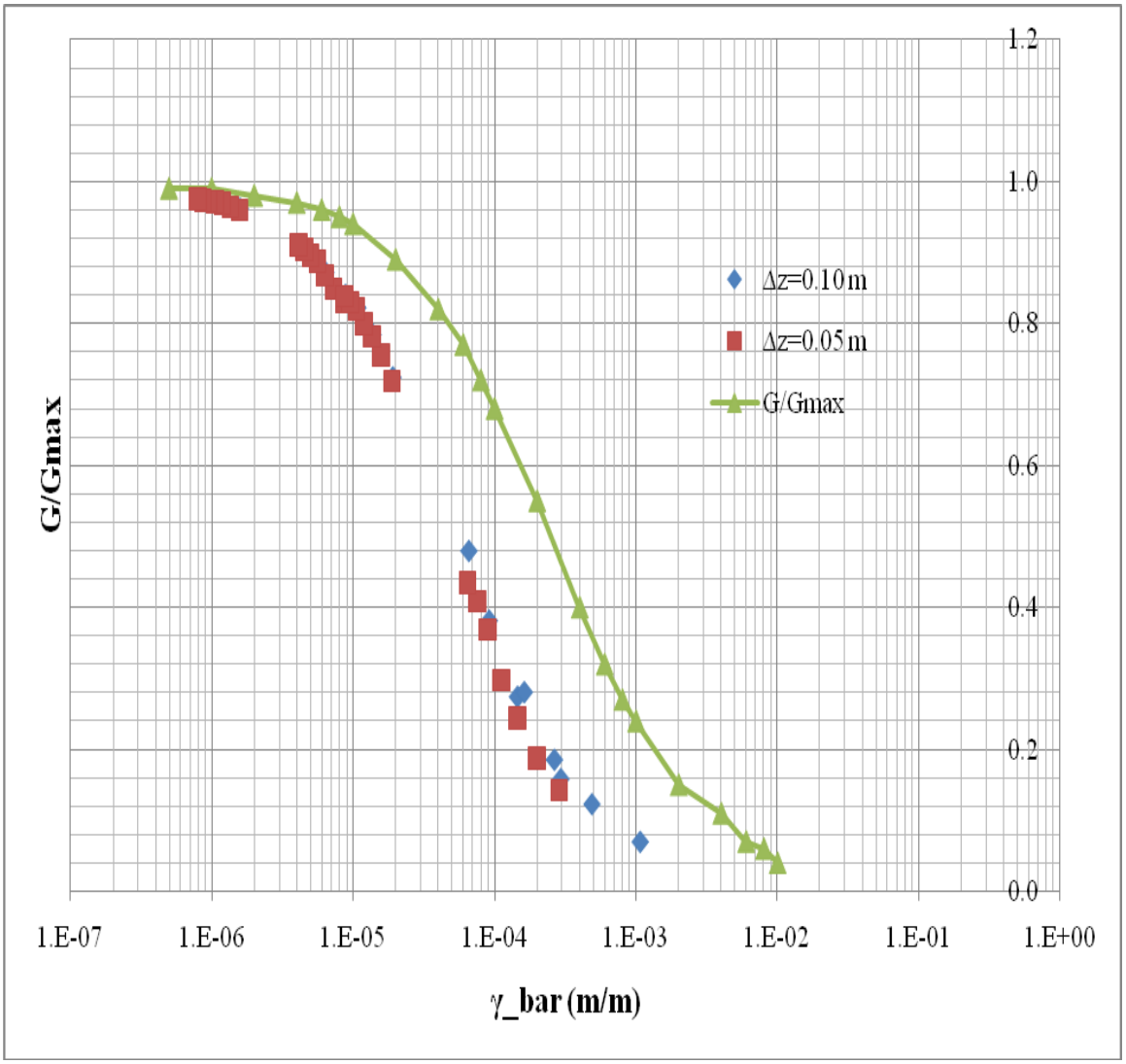

Figure 3.6 Shear Modulus Curve for $\frac{G}{G_{MAX}}$ vs. $\tilde{\gamma}$ with Δz=0.10 m and 0.05 m

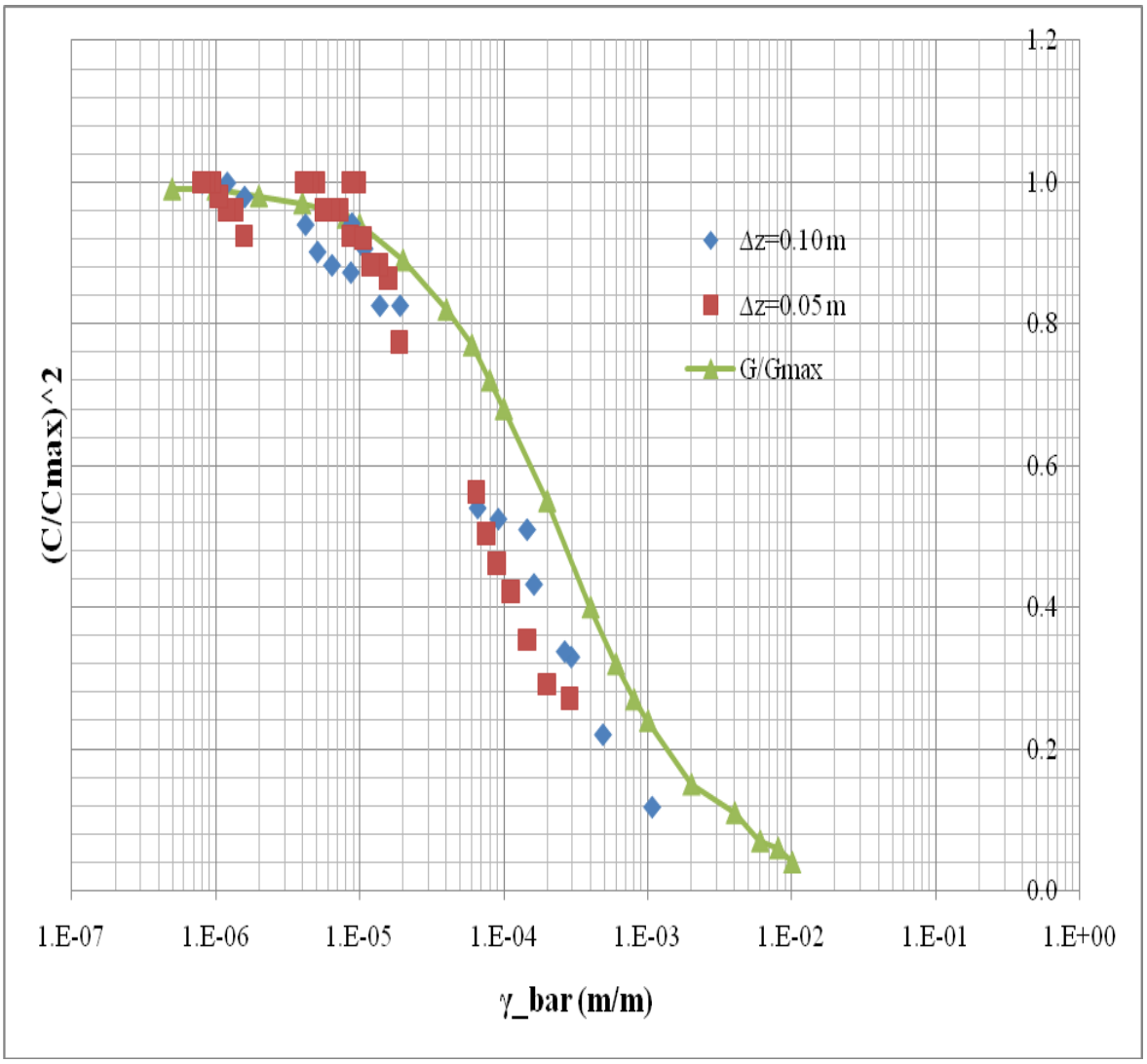

Figure 3.7 Shear Modulus Curve for $\frac{c^2}{c^2_{MAX}}$ vs. $\tilde{\gamma}$

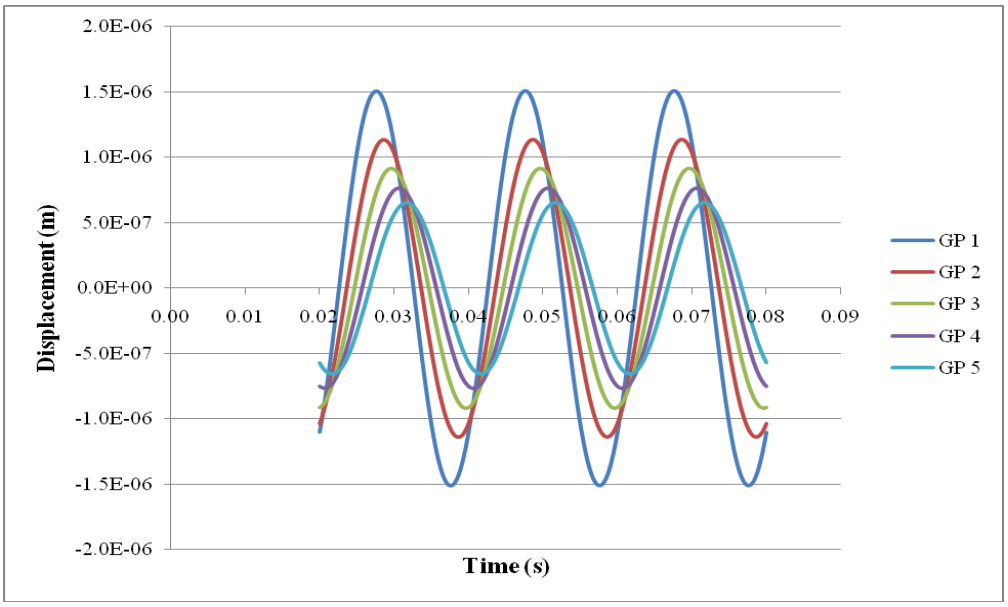

Figure 3.8 Displacement History--P=100 N with Δz= 0.10 m f= 50 Hz

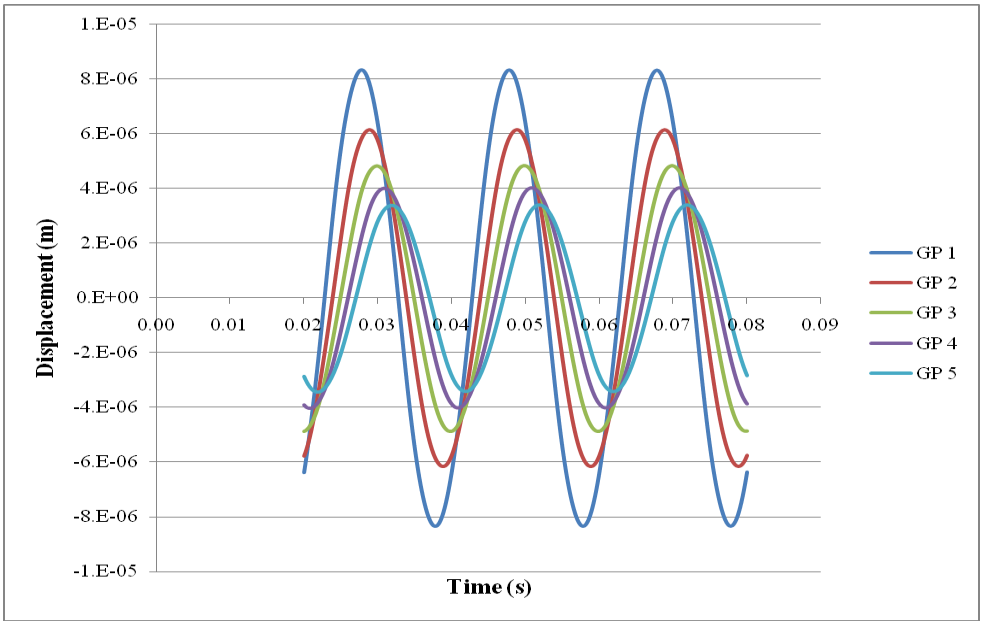

Figure 3.9 Displacement History--P=500 N with Δz= 0.10 m f= 50 Hz

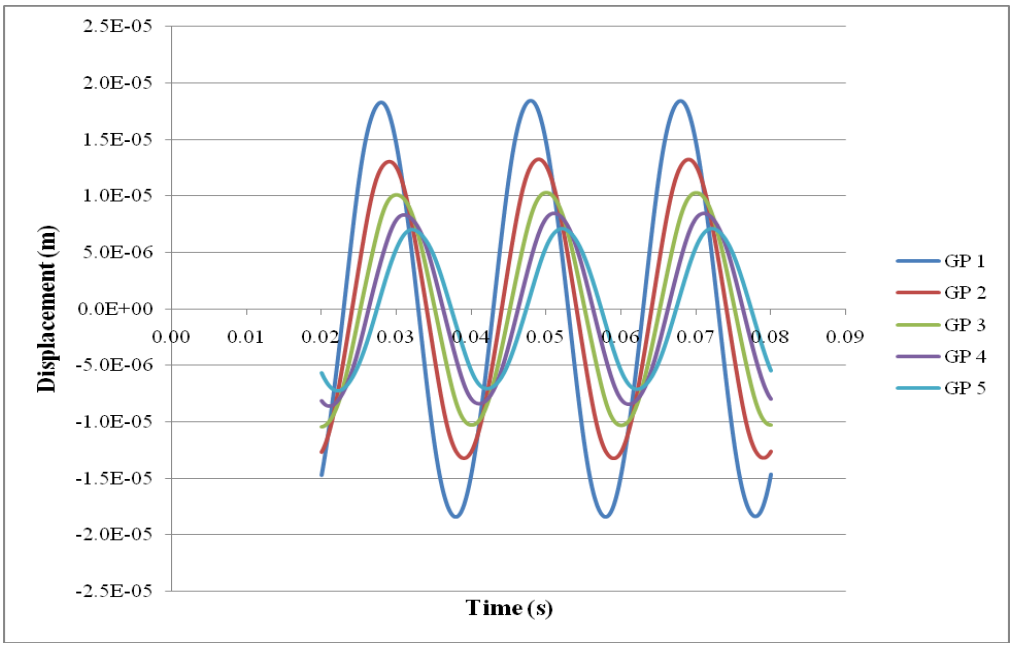

Figure 3.10 Displacement History--P=1,000 N with Δz= 0.10 m f= 50 Hz

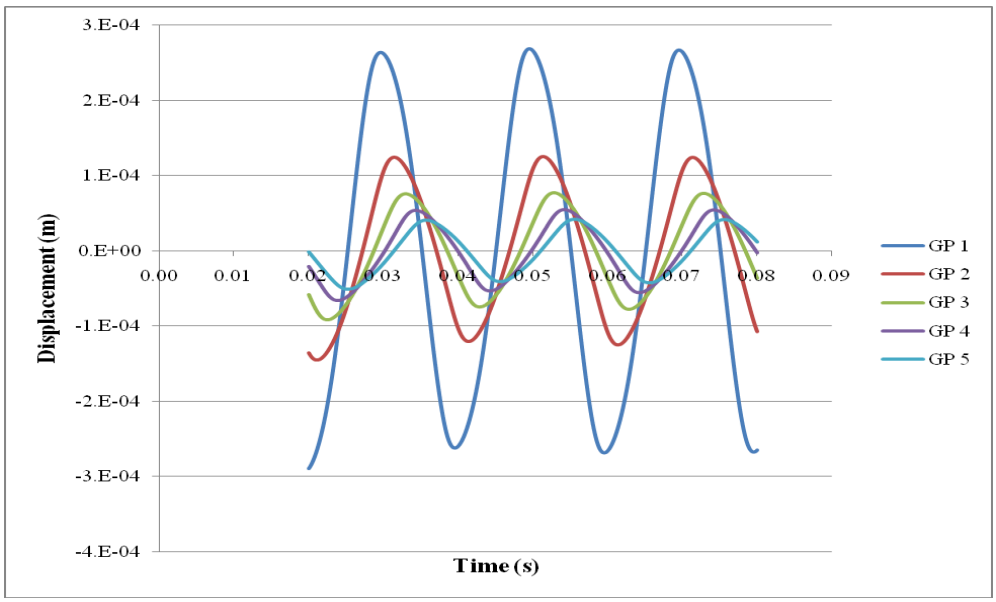

Figure 3.11 Displacement History--P=5,000 N with Δz= 0.10 m f= 50 Hz

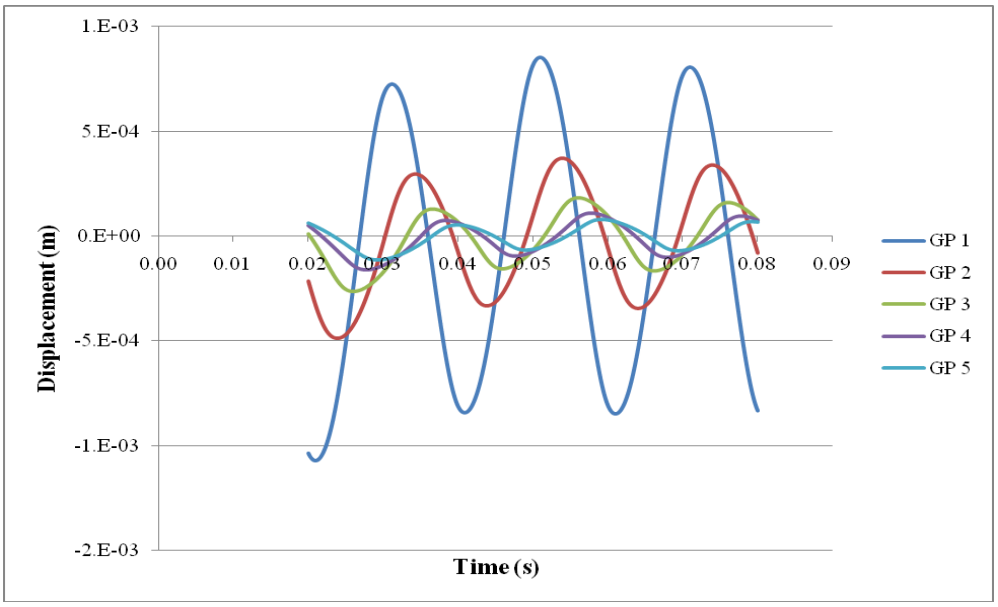

Figure 3.12 Displacement History--P=10,000 N with Δz= 0.10 m f= 50 Hz

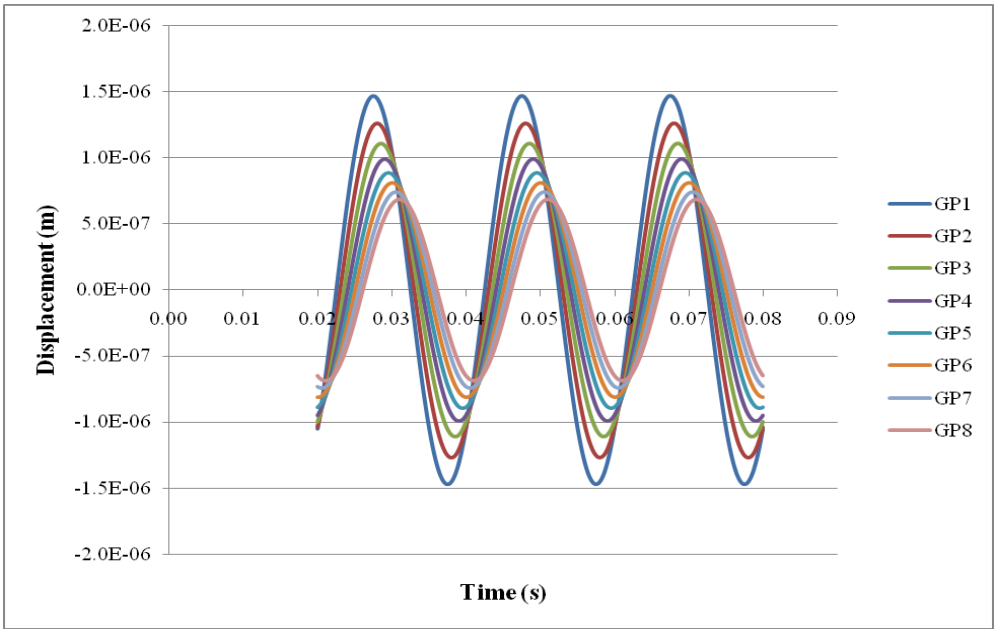

Figure 3.13 Displacement History--P=100 N with Δz= 0.05 m f= 50 Hz

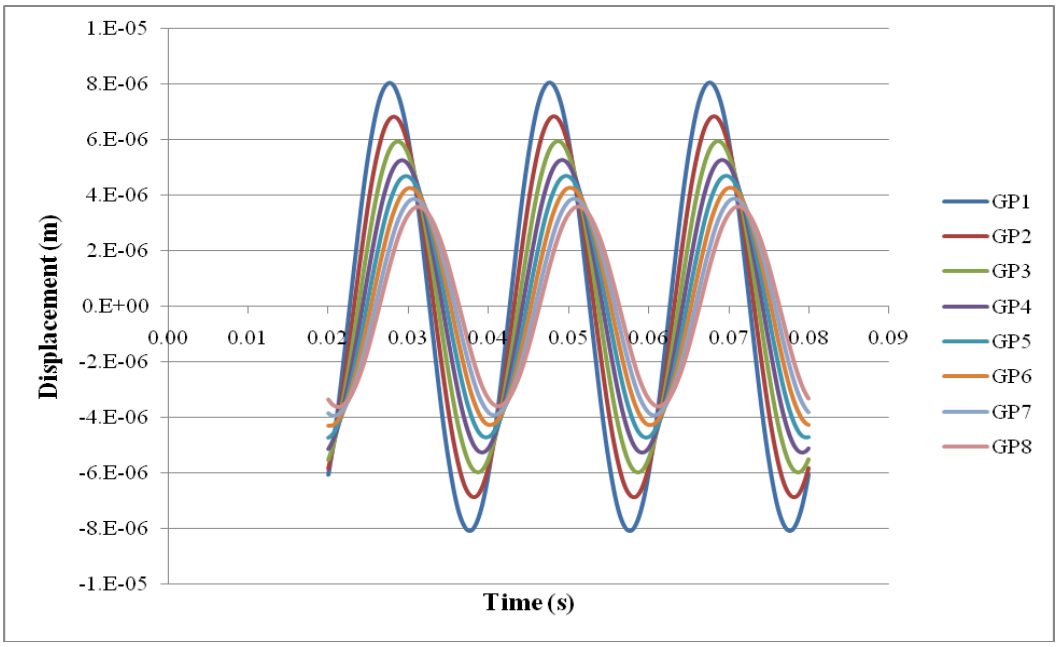

Figure 3.14 Displacement History--P=500 N with Δz= 0.05 m f= 50 Hz

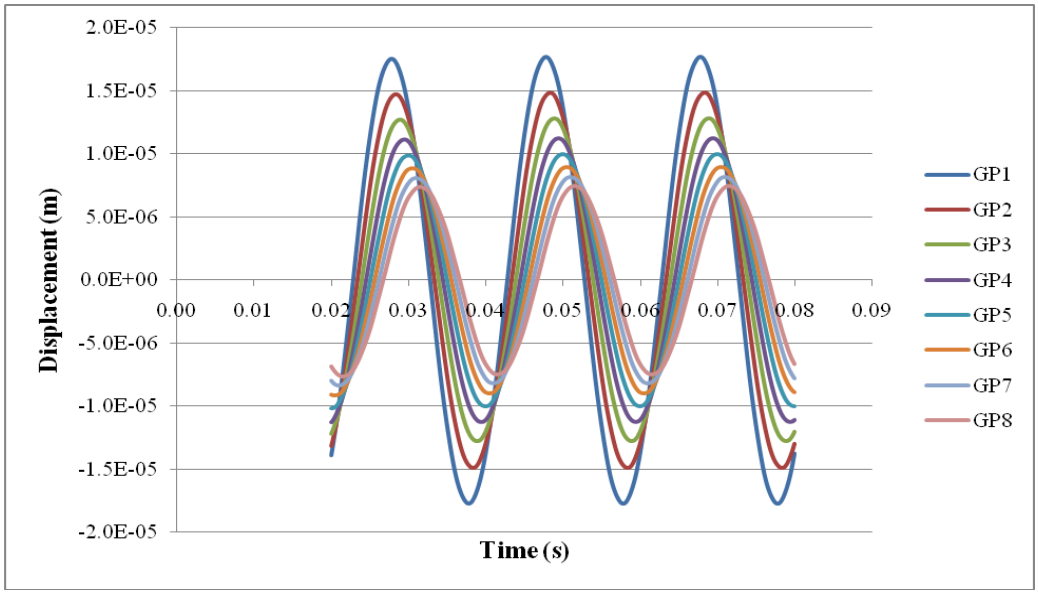

Figure 3.15 Displacement History--P=1,000 N with Δz= 0.05 m f= 50 Hz

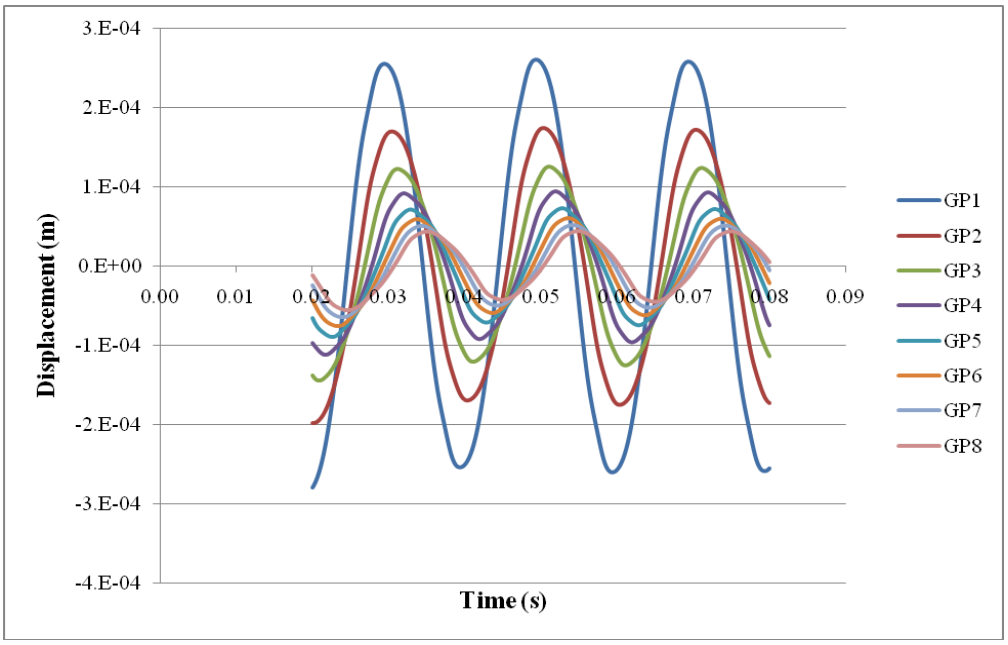

Figure 3.16 Displacement History--P=5,000 N with Δz= 0.05 m f= 50 Hz

4. CONCLUSIONS

4.1. Summary and Conclusions

The main objective of this study was to evaluate the accuracy of the procedure used in practice to determine soil properties in situ in order to compare them to those reported in the literature from lab tests.

For this purpose a shear cone that would reproduce correctly the horizontal stiffness of a circular mat foundation on the surface of an elastic, homogeneous half space, was considered. The cone was discretized using both a system of lumped masses and springs and a finite difference scheme using second-order central difference formulas, verifying that in the linear elastic range the results were accurate. A number of studies were conducted next increasing the level of the applied force and using nonlinear springs that would reproduce a specified G/G_{max} vs. γ curve. Using a similar procedure to that used in the field tests the shear wave velocity between hypothetical receivers and the levels of strain were determined. The resulting values of G/G_{max} vs. γ were then compared with the assumed curve to assess the accuracy of the estimated values.

For the springs model mesh sizes of 0.05, 0.10 and 0.20 m were considered. The displacement time histories were obtained at the surface, and at various depths for a frequency of 50 Hz.

Mesh sizes of 0.10, 0.05 and 0.01 m were considered for the finite difference using second-order central difference model. In order to get accurate results the mesh

size for the finite difference model had to be much smaller than the Δz used with the lumped masses and springs.

The values of the strains computed with the 3 models and from the analytical formula were compared next. Δz=0.10 m and Δz=0.05 m with the springs model and for finite differences with Δz=0.01 m. The results with springs and Δz=0.05 m and with finite differences and Δz=0.01 m were in very good agreement with the analytical solution. Those with Δz=0.10 m were slightly off.

Nonlinear Runs were performed with the springs model, Δz=0.10 m and Δz=0.05 m. The values of G/G_{MAX} versus γ obtained for both cases matched exactly from the direct computation of $G_{\max}$ and γ_{MAX} the assumed material curve. This verifies that the correct variation of G with γ is being used in the computer program (γ is the maximum shear strain computed by the program). The values of C^2/C^2_{MAX} squared were always larger than those of G/G_{MAX}. This indicates that the shear wave velocity computed is an average velocity over time rather than the minimum velocity corresponding to γ_{MAX}.

The shear strain computed from the maximum displacements $\tilde{\gamma}$ is always smaller than the actual γ_{MAX} and therefore the results with these values would be to the left of the experimental (assumed) curve.

Using the results of C^2/C^2_{MAX} versus $\tilde{\gamma}$ introduced 2 errors of opposite signs but the one associated with the use of $\tilde{\gamma}$ instead of the true γ_{MAX} is larger resulting therefore in a field curve that would be to the left (and below) the laboratory curve.

4.2 Further Studies

This work has shown that the procedures commonly used to obtain G/G_{MAX} vs. γ curves from field tests tend to introduce some errors. In this work only the effects of using the time difference between the occurrence of the maximum displacements at the receivers and of computing the shear strain on the difference between these maxima divided by the distance between receivers were investigated. The effects of using the one dimensional expression for the shear strain, neglecting the vertical displacements that would take place in the tests (unless the receivers were placed at the center line), and the difference between using the horizontal shear strain or the octahedral one should be further investigated. This requires, however using 3D models.

REFERENCES

Ahn, J. (2007) "In situ determination of dynamic soil properties under an excited surface foundation," Ph.D. dissertation, The Dwight Look College of Engineering, Texas A&M Univ., College Station, TX.

Anderson, D. G. and Woods, R. D. (1975). "Comparison of field and laboratory shear modulus." *Proc. ASCE Conference on In-Situ Measurements of Soil Properties,* Vol. I, 69-62.

Darendeli, M. B. (2001). "Development of a new family of normalized modulus reduction and material damping curves," Ph.D. dissertation, Cockrell School of Engineering, The University of Texas, Austin, TX.

Iwan, W. D. (1967). "On a class of models for the yielding behavior of continuous and composite systems." *J. of Appl. Mech.,* 34(3), 612-617.

Kausel, E. (1974). "Forced vibration of circular foundations on layered media," Ph.D. dissertation, School of Engineering, Massachusetts Institute of Technology, Cambridge, MA.

Kim, D-S. (1991). "Deformation characteristics of soils at small to intermediate strains from cyclic tests," Ph.D. dissertation, Cockrell School of Engineering, The University of Texas, Austin, TX.

Luco, J.E. and Westmann, R. A. (1971). "Dynamic response of circular footings." *J. of the Engin. Mech. Div.,* 97, 1381-1395.

Park, K. (2007). "Field measurement of the linear and nonlinear shear moduli of soils using dynamically loaded surface footings," Ph.D. dissertation, Cockrell School of Engineering, The University of Texas, Austin, TX.

Seed, H. B. and Idriss, I. M. (1970). "Moduli and damping factors for dynamic response analysis." *Report No. EERC 70-10,* University of California, Berkeley.

Stokoe, K. H., Kurtulus, A., and Park, K. (2006). "Development of field methods to evaluate the nonlinear shear and compression moduli of soil." *Earthquake Geotechnical Engineering Workshop,* Christchurch, New Zealand.

Veletsos, A. S. and Verbic, B. (1974). "Basic response functions for elastic foundations." *J. of the Engin. Mech. Div., (100), 189-202.*

Veletsos, A. S. and Wei, Y. T. (1971). “Lateral and rocking vibrations of footings.” *J. of the S. Mech. and Found. Div., (97), 1227-1248.*

APPENDIX

TOR1

```
C*************************************************
      PROGRAM TORRES1
C PROGRAM TO SOLVE SYSTEM OF NONLINEAR SPRINGS AND MASSES
REPRESENTING
C A CONE TO DETERMINE VARIATION OF MODULUS WITH STRAIN
      IMPLICIT REAL*8(A-H,O-Z)

      DIMENSION AK(50),FY(50),AM(1000),U(1000),U1(1000),U2(1000)
        DIMENSION ESP1(1000),GSM(1000),GM(1000),ESPM(1000),FOR(1000)
        DIMENSION F(50,1000),ESP(1000),AR(1000)
      COMMON AK,FY
        OPEN(2,FILE='SPSOIL',STATUS='OLD')
        READ(2,*)NSP
        DO 1 I=1,NSP
    1 READ(2,*)AK(I),FY(I)

      WRITE(*,*)' ENTER CS RHO DAMP'
      READ(*,*)CS,RHO,DS
      GS=RHO*CS*CS
```

```
WRITE(*,*)' ENTER RAD ZO DZ NLAY ICOD '
    READ(*,*)RO,ZO,DZ,NLAY,ICOD
NL1=NLAY+1
OPEN(1,FILE='TGGAM',STATUS='UNKNOWN')
OPEN(3,FILE='TU',STATUS='UNKNOWN')
OPEN(4,FILE='GGAM',STATUS='UNKNOWN')



PI=3.1415926535
    ARO=PI*RO*RO
    ZZ2=ZO*ZO
    ARZ=ARO/ZZ2
    AM(1)=0.
    DO 2 I=1,NLAY
U(I)=0.
    U1(I)=0.
    U2(I)=0.
    ESP(I)=0.
    ESPM(I)=0.
    FOR(I)=0.
    GSM(I)=0.
    DO 3 J=1,NSP
```

```
      F(J,I)=0.
3 CONTINUE
  Z1=ZO+(I-1)*DZ
      Z2=Z1+DZ
      R=RO*Z2/ZO
      R1=RO*Z1/ZO
      AREQ=ARZ*Z1*Z2
      AMI=RHO*ARO*DZ/6./ZZ2
      IF(ICOD.NE.0)GO TO 4

      AMT=AMI*(Z2*Z2+Z2*Z1+Z1*Z1)

      AR(I)=AREQ*GS
      AM(I)=AM(I)+AMT
  AM(I+1)=AMT
      GO TO 2
4 Z2=Z1+DZ/2.
  REQ=RO*Z2/ZO

      AR(I)=AREQ*GS
  AMT=AMI*(Z2*Z2+Z2*Z1+Z1*Z1)
      AM(I)=AM(I)+2.*AMT
```

```
 Z1=Z2
      Z2=Z1+DZ/2.
      AMT=AMI*(Z2*Z2+Z2*Z1+Z1*Z1)
      AM(I+1)=2.*AMT

2 CONTINUE
 AKB=5.*GS*R
      CB=0.6*AKB*R/CS
      AR(NL1)=1.
      WRITE(*,*)'ENTER P OM DT'
      READ(*,*)P,OM,DT
      WRITE(*,*)'ENTER NTI,NT'
      READ(*,*)NTI,NT
      DT2=DT*DT
      PER=1./OM
      OM=2.*PI*OM
      NTI=NTI*PER/DT
      NT=NT*PER/DT
      DO 1000 IT=1,NT
      T=IT*DT
 OMT=OM*T
      SS=DSIN(OMT)
```

```
      PP=P*SS
      U(1)=2.*U1(1)-U2(1)+DT2*(PP-AR(1)*FOR(1))/AM(1)
   FOR(NL1)=AKB*U1(NL1)+CB*(U1(NL1)-U2(NL1))/DT
      DO 10 J=2,NL1
 10 U(J)=2.*U1(J)-U2(J)-DT2*(AR(J)*FOR(J)-AR(J-1)*FOR(J-1))/AM(J)
   DO 11 J=1,NLAY
      ESP1(J)=ESP(J)
      ESP(J)=(U(J)-U(J+1))/DZ
   CALL FORCE(ESP,ESP1,F,FOR,NSP,J,GM)
      EP=DABS(ESP(J))
      IF(EP.GT.ESPM(J))GSM(J)=GM(J)
   IF(EP.GT.ESPM(J))ESPM(J)=EP
      U2(J)=U1(J)
 11 U1(J)=U(J)
   IF(IT.GT.NTI)WRITE(1,100)T,(ESP(J),GM(J),J=2,4)
      IF(IT.GT.NTI)WRITE(3,101)T,(U(J),J=1,5)
1000 CONTINUE
   WRITE(4,101)(ESPM(J),GSM(J),J=2,4)
 100 FORMAT(7E12.4)
 101 FORMAT(6E12.4)

   CLOSE(1)
```

```
      CLOSE(2)
          CLOSE(3)
      CLOSE(4)
      END
C*************************************************************
      SUBROUTINE FORCE(ESP,ESP1,F,FOR,NSP,IND,GM)
      IMPLICIT REAL*8(A-H,O-Z)
       DIMENSION F(50,1000),ESP(1000),ESP1(1000),FOR(1000),GM(1000)
      COMMON AK(50),FY(50)
          FOR(IND)=0.
          DO 10 JOSE =1,NSP
          FN=F(JOSE,IND)+AK(JOSE)*(ESP(IND)-ESP1(IND))
          FFN=DABS(FN)
          IF(FFN.GT.FY(JOSE))FN=FY(JOSE)*FN/FFN
          FOR(IND)=FOR(IND)+FN
   10 F(JOSE,IND)=FN
      GM(IND)=FOR(IND)/ESP(IND)
          RETURN
          END
```

TOR1A

TOR2

```
C**************************************************
      PROGRAM TORRES2
C PROGRAM TO SOLVE  NONLINEAR SHEAR CONE USING FINITE
DIFFERENCES USING SECOND-ORDER CENTRAL DIFFERENCE
C  TO DETERMINE VARIATION OF MODULUS WITH STRAIN
      IMPLICIT REAL*8(A-H,O-Z)

      DIMENSION AK(50),FY(50),AM(1000),U(1000),U1(1000),U2(1000)
         DIMENSION ESP1(1000),GSM(1000),GM(1000),ESPM(1000),FOR(1000)
         DIMENSION F(50,1000),ESP(1000),AR(1000),GAR(1000),UMAX(1000)
         DIMENSION TMAX(1000)
         COMMON AK,FY
         OPEN(2,FILE='SPSOIL',STATUS='OLD')
         READ(2,*)NSP
         DO 1 I=1,NSP
    1 READ(2,*)AK(I),FY(I)

      WRITE(*,*)' ENTER CS RHO '
      READ(*,*)CS,RHO
      GS=RHO*CS*CS
```

```
WRITE(*,*)' ENTER RAD ZO DZ NLAY  '
    READ(*,*)RO,ZO,DZ,NLAY
NL1=NLAY+1
    DZ2=2.*DZ
    DZZ=DZ*DZ
    UI=0.
OPEN(1,FILE='TGGAM2',STATUS='UNKNOWN')
OPEN(3,FILE='TU2',STATUS='UNKNOWN')
OPEN(4,FILE='GGAM2',STATUS='UNKNOWN')


PI=3.1415926535
    ARO=PI*RO*RO
    ZZ2=ZO*ZO
    ARZ=ARO/ZZ2

    DO 2 I=1,NL1
U(I)=0.
    U1(I)=0.
    U2(I)=0.
    ESP(I)=0.
    ESPM(I)=0.
```

```
      UMAX(I)=0.
      FOR(I)=0.
      GSM(I)=0.
      DO 3 J=1,NSP
      F(J,I)=0.
3 CONTINUE
  Z1=ZO+(I-1)*DZ
      Z2=Z1+DZ
      R=RO*Z2/ZO
      R1=RO*Z1/ZO
      AREQ=ARZ*Z1*Z2


      GAR(I)=AREQ*GS
      AR(I)=GAR(I)
      AM(I)=RHO*AREQ


2 CONTINUE


      WRITE(*,*)'ENTER P OM DT'
      READ(*,*)P,OM,DT
```

```
      WRITE(*,*)'ENTER NTI,NT'
      READ(*,*)NTI,NT
      DT2=DT*DT
      PER=1./OM
      OM=2.*PI*OM
      NTI=NTI*PER/DT
      NT=NT*PER/DT
C     NT=2
      DO 1000 IT=1,NT
      T=IT*DT
    OMT=OM*T
      SS=DSIN(OMT)
      PP=P*SS
      ESP1(1)=ESP(1)
      ESP(1)=PP/AR(1)
C     WRITE(3,101)ESP(1)
    DO 11 J=1,NLAY
      IF(J.GT.1)ESP1(J)=ESP(J)

      IF(J.GT.1)ESP(J)=(U1(J-1)-U1(J+1))/DZ2
    CALL FORCE(ESP,ESP1,F,FOR,NSP,J,GM)
```

```
      AR(J)=GM(J)*GAR(J)


          EP=DABS(ESP(J))
          IF(EP.GT.ESPM(J))GSM(J)=GM(J)
        IF(EP.GT.ESPM(J))ESPM(J)=EP
   11 CONTINUE
          UI=U1(2)+DZ2*PP/AR(1)
          ARI=3.*AR(1)-3.*AR(2)+AR(3)
          US=AR(1)*(2.*U1(2)-2.*U1(1)+DZ2*PP/AR(1))/DZZ
          UV=PP*(3.*AR(1)-4.*AR(2)+AR(3))/DZ2/AR(1)

C       WRITE(3,101)GM(1),AR(1),AM(1)
C       WRITE(3,101)ARI,US,UV
          U(1)=2.*U1(1)-U2(1)+DT2*(US+UV)/AM(1)


          DO 10 J=2,NLAY
          US=AR(J)*(U1(J+1)-2.*U1(J)+U1(J-1))/DZZ
          UV=(AR(J+1)-AR(J-1))*(U1(J+1)-U1(J-1))/DZ2/DZ2
   10 U(J)=2.*U1(J)-U2(J)+DT2*(US+UV)/AM(J)
        DO 13 J=1,NLAY
          U2(J)=U1(J)
   13 U1(J)=U(J)
```

```
      IF(IT.GT.NTI)WRITE(1,100)T,(ESP(J),GM(J),J=1,31,10)


          IF(IT.GT.NTI)WRITE(3,101)T,(U(J),J=1,41,10)
 1000 CONTINUE
      WRITE(4,101)(ESPM(J),GSM(J),J=1,41,10)
  100 FORMAT(9E12.4)
  101 FORMAT(6E12.4)


      CLOSE(1)
      CLOSE(2)
          CLOSE(3)
      CLOSE(4)
      END
C*************************************************************
      SUBROUTINE FORCE(ESP,ESP1,F,FOR,NSP,IND,GM)
      IMPLICIT REAL*8(A-H,O-Z)
       DIMENSION F(50,1000),ESP(1000),ESP1(1000),FOR(1000),GM(1000)
      COMMON AK(50),FY(50)
          FOR(IND)=0.
          DO 10 JOSE =1,NSP
          FN=F(JOSE,IND)+AK(JOSE)*(ESP(IND)-ESP1(IND))
          FFN=DABS(FN)
```

```
      IF(FFN.GT.FY(JOSE))FN=FY(JOSE)*FN/FFN
      FOR(IND)=FOR(IND)+FN
   10 F(JOSE,IND)=FN
     GM(IND)=1.
      EP=ESP(IND)
      EP=DABS(EP)
     IF(EP.GT.1.E-6)GM(IND)=FOR(IND)/ESP(IND)
C     IF(IND.EQ.1)WRITE(3,*)FOR(1),GM(1)
      RETURN
      END
```

VITA

Daniel E.Torres received his Bachelor of Science degree in civil engineering from Texas A & M University in 2006. He entered the structural engineering program at Texas A&M University in September 2009 and received his Master of Science degree in December 2010. His research interests include Finite Element Modeling, Structural Mechanics and Dynamics, Earthquake Engineering and Offshore Structures. His experience covers 2 ½ years in field and design engineering in the Oil and Gas Industry.

Daniel plans to pursue a career as a professional structural engineer and become a licensed engineer for the State of Texas.

Mr. Torres may be reached at 3136 TAMU, College Station, TX 77843. His email is tor40664@gmail.com.